Research Square

Preprints are preliminary reports that have not undergone peer review.
They should not be considered conclusive, used to inform clinical practice,
or referenced by the media as validated information.

Underlying histopathology features of white matter hyperintensities in vascular and neurodegenerative disorders: a systematic review

Eve-Marie Frigon

eve-marie.frigon@uqtr.ca

McGill University https://orcid.org/0009-0000-4396-6890

Amelie Metz

McGill University

Olivier Parent

McGill University

Katherine Chadwick

McGill University

Farooq Kamal

McGill University

Zaki Alasmar

McGill University

Aliza Brzezinski-Rittner

McGill University

Roqaie Moqadam

University of Montreal

Shima Raeesi

McGill University

Narges Taghizadehsalehabad

McGill University

Yashar Zeighami

yashar.zeighami@mcgill.ca

McGill University

Mahsa Dadar

mahsa.dadar@mcgill.ca

McGill University

Systematic Review

Keywords: white matter lesions, Alzheimer's disease, histology, demyelination, axonal damage, neuroinflammation, vascular pathology, magnetic resonance imaging

Posted Date: September 20th, 2026

DOI: https://doi.org/10.21203/rs.3.rs-11053221/v1

License: This work is licensed under a Creative Commons Attribution 4.0 International License. Read Full License

Additional Declarations: The authors declare no competing interests.

Abstract

White matter hyperintensities (WMHs) are a hallmark of cerebral small vessel disease, commonly seen in cognitively normal older adults and patients with neurodegenerative disorders, and are thought to reflect varying degrees of tissue damage. Although FLAIR and T2-weighted MRI remain the best modalities for detecting WMHs, these lesions cannot be reliably distinguished macroscopically from normal appearing white matter, so standard neuropathology protocols do not specifically consider WMH regions unless MRI guidance is available. As a result, histopathological data on WMHs from gold-standard studies remain limited relative to their clinical prevalence. This review aimed to evaluate existing evidence linking MRI-defined WMHs to their underlying histopathology in postmortem brains from patients with various neurodegenerative disorders and aging controls. After a PubMed literature search and screening of abstracts and full texts, we included 45 articles: 10 on normal aging, 16 on Alzheimer's disease, 10 on vascular dementia, and 9 on related conditions. WMHs were histopathologically characterized by myelin loss (including spongiosis), axonal rarefaction, edema, dilated perivascular spaces, gliosis, arteriolosclerosis, and venous collagenosis, all indicative of underlying white matter pathology. The findings overall suggest that WMHs are pathologically heterogeneous, varying according to their anatomical location and distribution. Disease-specific differences in regional distribution, neuroinflammation, vascular pathology, and proteinopathy further contribute to their development and clinical significance, highlighting the need to consider both diagnosis and anatomical location when interpreting the pathological substrates of WMHs.

Highlights

● WMH histology shows myelin and axonal loss, inflammation, and vascular pathology.

● WMH pathology varies by anatomical location and across neurodegenerative disorders.

● Multiple staining types and large sample sizes are needed to elucidate WMH pathology.

Introduction

White matter hyperintensities (WMHs), also referred to as leukoaraiosis, are regions of hyperintense signal observed on T2-weighted or fluid-attenuated inversion recovery (FLAIR) magnetic resonance images (MRIs), in contrast with the surrounding normal-appearing white matter (NAWM). WMHs can appear in various white matter (WM) regions, especially around the lateral ventricles, classified as periventricular WMHs (pvWMHs), which can present as caps, lining, halo, or irregular lesions, reflecting the severity of WM damage [1]. WMHs can also occur within the subcortical WM, referred to as deep WMHs (dWMHs), which can be categorized as punctate, early confluent, or confluent lesions as defined by Fazekas et al. [1]. More recently, additional categorizations of WMHs have been proposed, namely juxtacortical or superficial WMHs [2–4], as well as anterior-posterior [5–7] or lobar [5, 8–10].

WMHs represent a core feature of cerebral small vessel disease (cSVD), along with lacunar infarcts (i.e., cavities containing cerebrospinal fluid [11]), blood-brain barrier (BBB) damage [12], enlarged perivascular spaces and cerebral microbleeds [13]. WMHs are frequently observed in cognitively normal older adults [14], as well as in patients with various neurodegenerative disorders (NDDs) [8], including Alzheimer's disease (AD) [15], Parkinson's disease [16], Lewy body dementia [17, 18], frontotemporal dementia [19], amyotrophic lateral sclerosis (ALS) [20], and vascular dementia (VaD) [2, 21]. During normal aging, the prevalence of mild-to-severe WMHs has been reported as approximately 50.9% among individuals aged 40–49 years [22] and can increase to 96.6% among those aged 60–69 years [23], with evidence suggesting that their prevalence may have increased over time [24]. Another study showed that the prevalence of all levels of WMHs (mild, moderate and severe) of 60 to 89 years old controls was 85.6%, while moderate-to-severe WMH prevalence was 36.7% [25]. The development and progression of WMHs have been associated with several vascular and lifestyle-related risk factors, including hypertension, heart disease, elevated homocysteine levels, diabetes, hypercholesterolemia, smoking, and high alcohol intake [26–30].

WMHs are important predictors for both stroke and dementia [22, 31]. They are associated with cognitive decline, impairment of executive functions and memory loss [32–36], as well as neuropsychiatric symptoms (e.g. increased risk of late onset depression) [37, 38]. They have also been associated with motor symptoms [39] such as freezing of gait in Parkinson's disease patients [40–42].

Regional WMHs present different underlying features and clinical outcomes. pvWMHs are stronger predictors of cognitive decline [24] and correlate more strongly with aging than dWMHs [43]. Although pvWMHs have been more extensively associated with clinical outcomes, dWMH burden may reflect a greater degree of demyelination than pvWMH burden [4, 24, 44, 45]. In addition, WMH development appears to follow a spatial gradient, with greater WMH volumes initially observed in the frontal lobe and then expanded to other lobes [4], although WMH distribution patterns can differ across disorders [8]. Greater frontal WMH burden has also been associated with more pronounced impairments in executive function [46, 47]. Finally, NAWM may not necessarily be structurally "normal" in brains with high WMH burden, as structural and vascular alterations can extend beyond the areas of visible WMHs on MRI [48–50]. Given that WMH burden differs in volume and location, the underlying pathology of these different lesion types is still not fully understood.

WMHs can reflect varying levels of tissue alterations including myelin loss, axonal rarefaction, edema, perivascular space dilation, gliosis, and microvascular abnormalities, such as arteriolosclerosis and venous collagenosis, all of which are indicative of WM tissue damage [51–57]. Earlier studies have reported that extensive WMHs are associated with reduced glial density and the presence of vacuoles [58], whereas less extensive WMHs have been associated with microglial and endothelial activation [59]. It remains unclear whether the location of WMHs and the underlying disease pathology influence the specific tissue alterations associated with WMH formation.

Significant advances in in vivo neuroimaging, particularly quantitative MRI (qMRI), have provided additional insights into the microstructural alterations associated with WMHs [60]. Compared with NAWM, WMHs are characterized by increased mean diffusivity and T1 relaxation times, as well as decreased fractional anisotropy and magnetization transfer ratio [61–65]. These quantitative MRI features can reflect loss of myelin (e.g. magnetization transfer ratio and myelin water fraction) and fiber integrity (e.g. fractional anisotropy), as well as edema (e.g. mean diffusivity). Finally, quantitative T2* has been proposed as a potential indicator of tissue damage within WMHs [4]. While qMRI measures of WMHs allow to infer microstructural alterations of WMHs, few studies have directly validated qMRI measures of WMHs against gold-standard postmortem staining.

In vivo or ex vivo MRIs are not always available to guide the study of WMHs on postmortem brain tissue using gold-standard histology, and WMHs cannot be reliably distinguished from NAWM macroscopically. Consequently, standard neuropathology protocols do not routinely sample WMH regions, resulting in relatively sparse evidence from gold-standard histopathological studies despite their high prevalence. Although some neuropathological markers associated with WMHs are relatively well established in the literature, such as amyloid and tau, there remains limited information regarding other biomarkers implicated in cSVD, such as neuroinflammation markers or vascular pathology. Their contributions, either as potential cause or outcomes of WMHs, remain to be elucidated (e.g., whether gliosis leads to demyelination or emerges as its consequence). Furthermore, as WMH categorization varies across studies and sampling protocols are often sparse (i.e. do not commonly include multiple blocks covering different brain regions), the distribution and severity of these markers within different WMH regions (i.e., dWMHs, pvWMHs, or NAWM surrounding the WMH boundaries) and their distinct patterns across NDDs remain poorly understood. Finally, it remains unclear how the histopathological features of WMHs differ between cognitively normal elderly, AD and other NDDs, and how these differences relate to the severity of cognitive impairment.

The primary goal of this review was to assess the available evidence linking WMHs identified through in or ex vivo brain MRIs and their underlying pathological features using gold-standard histology in postmortem brains from patients with different NDDs and aging controls. More specifically, we aimed to identify how often markers of neuroinflammation, demyelination, BBB integrity, vascular integrity, and axonal rarefaction were reported within WMH regions, and to evaluate the potential variability in their patterns across different NDDs and in different regions.

Methods

Inclusion and exclusion criteria

Peer-reviewed, full-length articles published in English between 1986 and 2026 (last 40 years) were included if the authors reported histology features of WMHs identified on MRI and quantified as an outcome, predictor, or co-variate. We included WMH studies that incorporated postmortem assessment or autopsy of stroke, CVD, VaD, Lewy body dementia, Frontotemporal dementia, AD, Parkinson's disease,

ALS, mixed dementia, or healthy aging, but excluded multiple sclerosis studies. We further excluded literature reviews, as well as animal, cell culture, or pediatric population studies.

Study selection

The initial literature search was conducted on March 10th 2026 (EMF) using PubMed with the following keywords and their synonyms: “white matter hyperintensities,” “histology,” “pathology,” “magnetic resonance imaging,” “neurodegeneration,” and “dementia.” This search identified 536 articles, which were imported into Rayyan for deduplication and screening by two independent reviewers (EMF and AM). Following title and abstract screening, the two reviewers reached consensus on the inclusion of 56 articles. These articles subsequently underwent full-text screening according to the eligibility criteria shown in Data extraction. A flowchart of the study selection is presented as Figure 1.

Data extraction

If the article met all criteria, three reviewers independently extracted the features of interest based on a standard template. An additional reviewer (EMF) was responsible for merging the reviewers’ assessments and resolving discrepancies to reach consensus. The data extraction form included (a) Study information: title, authors list, publication journal and year, country or region of the authors, study aims and hypotheses; (b) Population: sample size, diagnosis group, cohort, country or region of the brain bank, inclusion and exclusion criteria, study type (in vivo, autopsies, postmortem or in vivo to ex vivo correlations), co-pathologies investigated and mean age, sex, ethnicity and risk factors per group; (c) Postmortem variables: fixation duration, postmortem interval (PMI), fixation solution, tissue type and size of the blocks; (d) White matter hyperintensities assessment: scanner strength and manufacturer, sequence used to detect WMHs, quantification method (volumetric or scales), analysis (visual assessment, automated, semi-automated or manual), WMH processing (i.e., method for WMH analysis), pattern (confluent, multi-spots, punctate) and distribution (lobar, global, periventricular), time interval between MRI and pathology; (e) Histology: confirmed diagnosis, sampling (number of blocks, number of sections analyzed), regions of interest of the blocks, section thickness, staining type, antibodies and concentrations for immunohistochemistry (IHC), features assessed, quantification methods, histology figures quality (background intensity, cellular intensity, tissue quality); (f) Results: statistical analysis type, adjustments and corrections, main findings (according to our aims), effect size, confidence intervals, p-values, correlations with qMRI findings, and clinical outcomes; (g) Overall appreciation: general notes, strengths, weaknesses, what remained unclear after thorough assessment of the paper.

Figures

Figures 3-5 present data collected in our laboratory. Ethics approval for the study was obtained from the Ethics Review Board of the Douglas Research Center (2023-622). Postmortem human brain specimens were acquired from the Douglas Brain Bank (https://douglasbrainbank.ca/). Brain specimens were collected in accordance with informed consent of the donors or their next of kin, according to tissue

banking practices regulated by the Quebec Health Research Fund, and the Guidelines on Human Biobanks and Genetic Research Databases overseen by the Douglas Research Ethics Board [66].

Results

Included studies

Following thorough full-text assessments, eleven articles were excluded as they 1) did not include histopathological analyses (n = 9), 2) were case reports (n = 1), or 3) were methodology-related studies (n = 1) (Fig. 1). The final review therefore included 45 articles (Table 1), which were grouped according to the population or disease of interest: normal aging, AD, CVD or other types of dementia and NDDs. The distribution of WMHs examined in each study (e.g. periventricular, deep, or both), the types of histological stains used, and the assessed features (e.g. demyelination, axonal damage, neuroinflammation, or vascular pathology) are also summarized in Table 1.

Of the 45 included studies, 10 focused on normal aging (22.2%), 16 on AD (35.6%), and 10 on VaD (22.2%). The remaining 9 studies included subjects with mixed dementia (n = 4; 8.9%), dementia (n = 3; 6.7%), CADASIL (n = 1; 2.2%), or ALS (n = 1; 2.2%) (Fig. 2A). Among the 10 studies focusing on normal aging, only one reported correlation with clinical data (10%), three were based on autopsy cohorts (30%), and the remaining six only examined postmortem brain tissue (i.e. no in vivo information was included in the study; 60%). Among the 16 AD studies, three reported correlations with clinical data (18.75%), one was based on an autopsy cohort (6.25%), and the remaining 12 were exclusively ex vivo (75%). In the VaD group, half of the studies (n = 5) reported clinical data, while the other half (n = 5) studies were exclusively ex vivo; none of the VaD studies were based on autopsy cohorts. Finally, among the nine studies in the “Others” group, two reported clinical data (22.2%; one mixed dementia and one dementia study), two were based on autopsy cohorts (22.2%; one mixed dementia study and the CADASIL study), and five were exclusively ex vivo (55.6%) (Fig. 2B).

The main contributions of the 45 studies were categorized according to their assessment of four histopathological features: 1. Demyelination, including markers of myelin sheath and oligodendrocytes (Fig. 3A); 2. Axonal damage, including markers of neurofibrillary tangles and axonal morphology (Fig. 3B); 3. Neuroinflammation, including markers of astrogliosis, microglial activation, macrophages, and iron accumulation (Fig. 3C); and 4. Vascular pathology, including BBB disruption, arteriolosclerosis, venous collagenosis, vascular integrity, and iron accumulation (Fig. 3D). Among the 45 studies, 29 assessed demyelination (64.4%), 16 assessed axonal damage (35.6%), 22 assessed neuroinflammation (48.9%), and 31 assessed vascular pathology (68.9%) (Fig. 2C). Only one of the 10 aging studies assessed axonal damage, whereas only four of the 16 AD studies reported findings related to neuroinflammation. In the VaD group, only three studies assessed axonal damage, while the number of studies addressing the four main histopathological features was more evenly distributed in the “Others” group (Fig. 2D). Few studies evaluated all four histopathological features concurrently, with only one aging study, one AD study, one VaD studies, and two “Others” studies assessing all four domains

(Table 1). In addition, we aimed to evaluate the associations between histopathological findings and qMRI features, as in vivo qMRI metrics have provided valuable insights into the underlying microstructural characteristics of WMHs. Only three studies assessed qMRIs and their correlation with histology features, especially qT1, qT2, fractional anisotropy and mean diffusivity. Furthermore, two studies correlated histology features with FLAIR signal intensity.

Finally, 26 studies evaluated pvWMHs and 36 evaluated dWMHs, while two studies did not report the location of the tissue blocks (Fig. 2E). Among the aging studies, 7/10 studies assessed pvWMHs, 9/10 assessed dWMHs, while 6/10 assessed both regions. AD studies primarily focused on dWMHs (12/16), followed by pvWMHs (7/16). Only 5/16 studies compared both anatomical regions. VaD studies frequently assessed pvWMHs (6/10) or dWMHs (6/10), but only two studies assessed both at the same time. Finally, all of the studies in the “Others” group assessed dWMHs (9/9), while 6/9 also assessed pvWMHs (Fig. 2F, Table 1).

Table 1

Selected studies. Studies were grouped according to the NDD diagnostic. Study type (either in vivo, ex vivo or both), WMH regions of interest, staining types, and each article's main histopathology contributions are also reported.

Article	Groups	MRI	White matter regions of interest	Staining types	Main contribution
Al-Mashhadi et al., 2014	Aging (> 65 years)	Ex vivo	dWMHs	LFB, β-galactosidase, IHC of 8-OHdG, H2AX, DNA-PK, GFAP, Oligodendrocyte-specific protein, CD68, Collagen IV, P16, P53, P21	Neuroinflammation
Chimowitz et al, 1992	Aging (> 50 years)	Ex vivo	pvWMHs dWMHs	Modified Kluver-Barrera, Congo red, IHC of GFAP, Desmin	Demyelination Neuroinflammation Vascular pathology
Haller et al., 2013	Aging (> 70 years)	In vivo ↔ ex vivo	pvWMHs dWMHs Perivascular regions	Luxol-van Gieson	Demyelination
Moody et al., 1995	Aging (> 60 years)	Ex vivo	dWMHs (frontal, parietal, occipital lobes)	H&E, Alkaline Phosphatase (Bell and Scarrow), Modified Masson's trichrome	Vascular pathology
Moody et al., 2004	Aging (> 60 years)	Ex vivo	dWMHs (frontal, insular lobe)	Alkaline Phosphatase, Congo red, Masson's trichrome, Kultchitsky hematoxylin, LFB-Cresyl violet	Vascular pathology
Murray et al., 2012	Aging (> 70 years)	Ex vivo	pvWMHs dWMHs (occipital lobe) Splenium of the corpus callosum	LFB, H&E, IHC of MBP, neurofilament, GFAP, Iba1, Collagen-IV	Demyelination Axonal damage Neuroinflammation Vascular pathology

Article	Groups	MRI	White matter regions of interest	Staining types	Main contribution
Scarpelli et al., 1994	Aging (> 65 years)	Autopsies	pvWMHs (anterior, posterior) dWMHs (frontal, occipital lobe)	LFB, H&E, IHC of GFAP	Demyelination Neuroinflammation Vascular pathology
Simpson et al., 2007 (a)	Aging (> 65 years)	Autopsies	pvWMHs dWMHs	LFB, H&E, IHC of CD68, GFAP, PDGFαR, MAP-2, MBP, fibrinogen	Demyelination Neuroinflammation
Simpson et al., 2007 (b)	Aging (> 65 years)	Autopsies	pvWMHs dWMHs	LFB, H&E, IHC of HLA-DR, CD68, CD40, CD40L, Mcm-2, PCNA, Ki6, GFAP	Neuroinflammation
Smith et al., 2000	Aging (> 75 years)	Ex vivo	pvWMHs (anterior, posterior)	LFB	Demyelination
Desmarais et al., 2021	AD FTD	In vivo ↔ ex vivo	pvWMHs	LFB, H&E, IHC of Neurofilament, GFAP, CD68, Tau, p62, α-synuclein, TDP-43	Demyelination Axonal damage Neuroinflammation Vascular pathology
Gouw et al., 2008	AD	Ex vivo	pvWMHs dWMHs (prefrontal, frontal, parietal lobes)	LFB, H&E, Bodian silver, IHC of HLA-DR, GFAP	Demyelination Axonal damage Neuroinflammation
Grafton et al., 1991	AD	Ex vivo	Not reported	LFB, Holmes, Holzer, Gallocyanin, IHC of GFAP	Demyelination Axonal damage Neuroinflammation
Keith et al., 2017	AD	In vivo ↔ ex vivo	pvWMHs (anterior, middle, posterior levels)	LFB, H&E, Gomori, Masson's trichrome, IHC of smooth muscle actin, GFAP, CD68, neurofilament	Vascular pathology

Article	Groups	MRI	White matter regions of interest	Staining types	Main contribution
Littau et al., 2022	AD CADASIL	Ex vivo	dWMHs (frontal cortex, temporal cortex, parietal cortex, occipital cortex)	LFB, H&E , IHC of β-amyloid, PDGFRβ, AQP4, GFAP, fibrinogen	Demyelination Vascular pathology
Malla et al., 2025	AD	Ex vivo	dWMHs (frontal, occipital lobes)	LFB,, IHC of HSPA6, HSP90A1	Demyelination
McAleese et al., 2013	AD LBD	Ex vivo	dWMHs (prefrontal, frontal, temporal, parietal, occipital lobes)	LFB, H&E	Vascular pathology
McAleese et al., 2015	AD	Ex vivo	dWMHs (prefrontal, mid-frontal, entorhinal, temporal, parietal, occipital lobes)	H&E, IHC of Tau, β-amyloid	Vascular pathology
McAleese et al., 2017	AD	Ex vivo	dWMHs (parietal lobe)	LFB, H&E, Bielschowsky, IHC of SMI-32, β-amyloid, Tau	Demyelination Axonal damage Vascular pathology
McAleese et al., 2019	AD	Ex vivo	dWMHs (parietal lobe)	LFB, H&E, Bielschowsky, IHC of fibrinogen, Tau, β-amyloid	Axonal damage Vascular pathology
McAleese et al., 2021	AD	Ex vivo	dWMHs (frontal lobe)	LF, H&E, Bielschowsky, IHC of Tau, β-amyloid	Demyelination Axonal damage Vascular pathology
Munoz et al., 1993	AD	Ex vivo	Not reported	H&E, Congo Red, Chromoxane cyanin, Bielschowsky	Demyelination Vascular pathology

Article	Groups	MRI	White matter regions of interest	Staining types	Main contribution
Roseborough et al., 2020	AD CVD	Ex vivo	pvWMHs dWMHs (frontal lobe)	LFB, H&E, IHC of neurofilament	Demyelination Axonal damage
Roseborough et al., 2021	AD CVD	Ex vivo	pvWMHs dWMHs (frontal lobe)	LFB, H&E, Movat's pentachrome, IHC of smooth muscle actin, fibrinogen, RCA lectin, Olig2, NeuN	Vascular pathology
Scheltens et al., 1995	AD	Autopsies	pvWMHs (anterior, posterior) dWMHs (frontal, occipital lobes)	H&E, PTAH, Kluver-Barrera, Bodian, Congo red, Elastic van Gieson	Demyelination Neuroinflammation Vascular pathology
Shim et al., 2015	AD CVD	In vivo ↔ ex vivo	pvWMHs dWMHs	LFB, H&E, Bielschowsky IHC of β-amyloid, Tau, α-synuclein	Demyelination Vascular pathology
Chen et al., 2016	VaD	In vivo ↔ ex vivo	dWMHs (frontal, temporal, prefrontal, parietal lobes)	LFB, H&E, IHC of GFAP, ALDH1L1, DLL1, LC3, PARP1, Fibrinogen, β-amyloid	Demyelination Neuroinflammation
Fernando et al., 2004	VaD	Ex vivo	pvWMHs dWMHs (centrum semiovale)	LFB, H&E, IHC of ICAM-1/CD54, CD68, Collagen-IV	Demyelination Neuroinflammation Vascular pathology
Fernando et al., 2006	VaD	Ex vivo	pvWMHs dWMHs	LFB, H&E, IHC of CD68, Collagen IV, HIF1α, HIF2α, ICAM-1/CD54, MMP7, Ngb, NMBR, VEGFR2/Flk-1, β-amyloid	Neuroinflammation Vascular pathology
Freeze et al., 2022	CAA	In vivo ↔ ex vivo	dWMHs (frontal, temporal,	LFB, H&E, Prussian blue, IHC of β-amyloid	Demyelination Axonal damage

Article	Groups	MRI	White matter regions of interest	Staining types	Main contribution
			parietal, occipital lobes) Corpus callosum (genu, body, splenium)		Vascular pathology
Huss et al., 2022	SVD	In vivo ↔ ex vivo	pvWMHs	IHC of GFAP and CHI3L1	Neuroinflammation
Lauer et al., 2016	CAA	In vivo ↔ ex vivo	dWMHs (midfrontal, middle-superior temporal, inferior parietal, cingulate, entorhinal)	H&E, Congo red, IHC of β-amyloid	Vascular pathology
Makkinejad et al., 2024	CAA	In vivo ↔ ex vivo	dWMHs (frontal, temporal, parietal, occipital lobes)	LFB, H&E, IHC of β-amyloid, neurofilament, GFAP, CD68	Demyelination Axonal damage Neuroinflammation Vascular pathology
Sole-Guardia et al., 2023	SVD	Ex vivo	pvWMHs	H&E, IHC of Iba1, GFAP	Neuroinflammation Vascular pathology
Sole-Guardia et al., 2024	SVD	Ex vivo	pvWMHs	LFB, H&E, Polarized Light Imaging (PLI), IHC of neurofilament	Demyelination Axonal damage
Sole-Guardia et al., 2025	SVD	Ex vivo	pvWMHs	H&E, Masson's trichrome, IHC of GLUT1, smooth muscle actin, IgG, MMP9	Vascular pathology
Fazekas et al., 1993	Mixed	Autopsies	pvWMHs dWMHs	H&E, Masson's trichrome, Kluver Barrera	Demyelination Axonal damage Neuroinflammation Vascular pathology

Article	Groups	MRI	White matter regions of interest	Staining types	Main contribution
Hainsworth et al., 2017	Dementia	Ex vivo	dWMHs (frontal, parietal cortex)	IHC of fibrinogen, IgG, CD68, CD34, smooth muscle actin	Neuroinflammation Vascular pathology
Lahna et al., 2023	Dementia	Ex vivo	pvWMHs (anterior, posterior) dWMHs (anterior, posterior, cingulate gyrus, parietal lobe) Corpus callosum	LFB, H&E, IHC of GFAP, Iba1, vimentin	Demyelination Neuroinflammation
Lahna et al., 2022	Dementia	In vivo ↔ ex vivo	pvWMHs (anterior, middle and posterior superolateral) dWMHs (frontal, temporal, parietal, occipital lobes)	LFB, H&E, Masson's trichrome, IHC of Tau, β-amyloid, α-synuclein, TDP-43, ubiquitin, smooth muscle actin	Vascular pathology
Pallebage-Gamarallage et al., 2018	ALS	Ex vivo	dWMHs (precentral gyrus, postcentral gyrus, central sulcus, middle frontal gyrus, orbital gyri, gyrus rectus, cingulate gyrus, inferior frontal gyrus, primary visual cortex) Corticospinal tract, Corpus callosum and fornix	IHC for PLP, Ferritin, CD68, GFAP, Iba1, pTDP-43, SMI-311, SMI-312	Demyelination Axonal damage Neuroinflammation
Silbert et al., 2024	MCI	Ex vivo	pvWMHs (posterior	LFB, H&E, IHC of GFAP, vimentin,	Demyelination

Article	Groups	MRI	White matter regions of interest	Staining types	Main contribution
	AD VaD		lateral-ventricle horn, posterior lateral-ventricle surface, midline periventricular, anterior lateral-ventricle surface, anterior lateral-ventricle horn) dWMHs (temporal, parietal, frontal lobes)	AQP1, AQP4, Iba1	Neuroinflammation Vascular pathology
Van Swieten et al., 1991	Mixed	Ex vivo	pvWMHs (frontal, occipital lobes) dWMHs (frontal, occipital lobes)	LFB, H&E, Phosphotungstic acid haematoxylin, Periodic acid-Schiff, Elastica van Gieson, Congo red, Bodian	Demyelination Axonal damage Neuroinflammation Vascular pathology
Yamamoto et al., 2009	CADASIL VaD	Autopsies	dWMHs (temporal pole)	LFB, H&E, Cresyl Violet, IHC of smooth muscle actin, medin, collagen IV, GLUT1, MBP, amyloid precursor protein	Demyelination Axonal damage Vascular pathology
Young et al., 2008	Mixed	In vivo ↔ ex vivo	pvWMHs (frontal, parietal, occipital lobes) dWMHs (frontal, parietal, occipital lobes)	H&E, Periodic Acid–Schiff, Weil's myelin stain, IHC of MBP, CD31, GLUT5, APP, HLA-DR, IgG	Demyelination Axonal damage Vascular pathology

AD = Alzheimer's disease; FTD = Frontotemporal dementia; LBD = Lewy bodies' disease; CVD = Cerebrovascular disease; VaD = Vascular dementia; CAA = Cerebral amyloid angiopathy; SVD = Small vessel disease; ALS = Amyotrophic lateral sclerosis; MCI = Mild cognitive impairment; pvWMHs = Periventricular white matter hyperintensities; dWMHs = Deep white matter hyperintensities; LFB = Luxol Fast blue; H&E = Hematoxylin and Eosin; IHC = Immunohistochemistry.

Staining protocols

We also documented the staining methods used in each included study (Table 1). For the assessment of myelin loss and damage, the most used staining methods were Luxol Fast Blue (LFB) and immunohistochemistry (IHC) for myelin basic protein (MBP) (Fig. 3A). Other myelin-related markers, including proteolipid protein (PLP) and myelin oligodendrocyte glycoprotein, were also reported. For the assessment of axonal damage, Bielschowsky's silver staining and IHC for neurofilament (NF) were the two most widely used methods (Fig. 3B), along with other silver stains, such as Bodian staining, and antibodies targeting a range of SMI markers. These staining methods were primarily assessed by quantifying staining intensity using predefined thresholds or intensity-based measurements extracted through image-processing software [53, 57, 67–86] to assess the percentage of staining area [57, 59, 73, 74, 79, 81, 84, 86–91].

Common indicators of neuroinflammation include glial cells, for which IHC markers such as glial fibrillary acidic protein (GFAP) for astrocytes and ionized calcium-binding adaptor molecule 1 (Iba1) for microglia were frequently used (Fig. 3C). Iba1 is a widely used marker of microglia and can identify both activated and non-activated microglia, with their activation state generally inferred from morphological characteristics. CD68 was also frequently reported in studies assessing macrophages. Some studies quantified cell bodies or used stereological approaches to assess cell density [58, 67, 69, 76, 78, 80, 81, 83, 84, 92, 93], whereas others used semi-quantitative visual scoring [53, 56, 59, 70, 78, 80–82, 87, 91, 93–102].

For the assessment of vascular pathology, hematoxylin and eosin (H&E) was the most commonly used stain, with endothelial cell characteristics and vessel wall thickness frequently quantified. H&E was also the primary general neuropathological stain used to assess overall tissue integrity in both NAWM and WMH regions. As shown in Fig. 3D, Masson's trichrome staining, which stains tissue fibers red/pink and collagen blue, was frequently used in studies of vascular pathology to assess blood vessel walls. Other markers, including IHC for collagen-IV and smooth muscle actin, were also used to differentiate arteries from veins, allowing for their separate assessment within WMH regions.

Demyelination Patterns

Radiological WMH scores are associated with corresponding neuropathological scores reflecting severity of demyelination [44, 82]. Myelin pallor is also identified as a major contributor to T2

hyperintensity [95], and correlated with decreased fractional anisotropy and increased mean diffusivity within WMH regions compared to NAWM [77, 97]. Demyelination has therefore been described as the main underlying feature of WMHs, where both periventricular and deep WMHs are associated with substantial myelin loss, as indicated by reduced myelin basic protein (MBP) [80] or LFB [79, 99] staining, as well as vacuolated myelin and vascular alterations [103].

In two patients with AD, Munoz et al. reported a reduction in myelinated fiber density, diffuse WM vacuolation (spongiosis), and decreased oligodendroglial nuclear density in extensive WMHs [58]. These findings were also observed in the WMH sections shown in Fig. 3, including MBP (Fig. 3A), Bielschowsky (Fig. 3B), and H&E and Masson's trichrome staining (Fig. 3D). However, the authors also reported that punctate WM changes are associated with enlarged perivascular spaces but do not appear to correlate with WM pallor [58].

Regional Differences in Demyelination

As pvWMHs are considered to be more strongly associated with aging and dWMHs exhibiting myelin degeneration are thought to be more closely associated with other underlying brain pathologies [103], several studies have investigated the patterns of WMH demyelination according to their location (i.e., periventricular or deep). The distribution patterns of WMHs are linked to specific underlying neuropathological features [95]. Myelin pallor is most strongly associated with caps (i.e., pvWMHs), while rims are associated with subependymal gliosis [95, 104]. Furthermore, punctate lesions are associated with dilated perivascular spaces or perivascular gliosis, and patch-like lesions are associated with myelin pallor [95]. Fazekas and his team later described the same pattern, categorizing dWMHs into punctate, early confluent, and confluent, corresponding to increasing severity of ischemic tissue damage [1]. Irregular pvWMHs show similar ischemic changes to confluent dWMHs, including myelin degeneration and fiber loss. Caps and smooth halo of pvWMHs are predominantly linked to nonischemic changes associated with demyelination [1].

Murray et al. similarly reported that MBP staining is reduced in dWMHs compared to NAWM, with an even greater reduction observed in pvWMHs. They also found a lower density of oligodendrocyte cell bodies in pvWMHs compared with NAWM, whereas oligodendrocyte density remains unchanged in dWMHs [76]. Another study examining demyelination reported a higher density of remyelinating oligodendrocytes in pvWMHs than in dWMHs, particularly within the perilesional rim rather than the lesion core [80]. NAWM proximal to WMHs shows similar but milder abnormalities that diminish with distance from WMHs [79]. In addition, WM rarefaction, axonal damage, and demyelination are observed beyond the lesion core, suggesting that pathological alterations extend into the surrounding tissue [97].

Demyelination in AD and other NDDs

In a study comparing WMHs in AD and frontotemporal dementia, the majority of cases exhibit moderate-to-severe myelin pallor in pvWMH blocks, regardless of diagnosis [96]. Similarly, a study comparing AD patients with controls reported that LFB staining is reduced within WMHs in both groups [89], and that

this reduction is associated with longer T1 relaxation times [53]. dWMHs are also associated with a loss of myelinated axons, even when lesions appear mild on MRI [70]. Demyelination is identified as the primary pathological substrate of WMHs in both AD patients and controls, although AD brains have a greater WMH volume than controls [91, 101]. However, McAleese et al. reported that WMH severity is associated with both axonal loss and demyelination in AD, whereas only demyelination appears to be the predominant pathological feature in control specimens [75]. Overall, they also found significantly greater demyelination in WMH tissue compared to NAWM [74].

Roseborough et al. assessed 20 specimens, including five AD, five CVD, five CVD + AD, and five controls [57]. They found that pvWMHs exhibit significant myelin loss compared to NAWM, as reflected by a reduced LFB field fraction, which significantly correlates with T1, FLAIR, and T2 signal intensities. However, ROI-averaged MRI intensities do not reliably correlate with histological tissue loss when pvWMHs and NAWM are analyzed separately, suggesting that WMH signal intensity alone may not accurately reflect the severity of myelin loss. The study also demonstrated that NAWM in AD and CVD specimens exhibit higher FLAIR signal intensity than NAWM in controls, suggesting that pathological alterations may extend beyond the visible boundaries of WMHs. Finally, pvWMHs in specimens with comorbid AD and CVD do not exhibit an additive increase in myelin loss compared with those associated with either CVD or AD alone [57].

In patients with post-stroke dementia and those without dementia, the myelin index is lower compared to controls, reflecting greater severity of dWMHs [67]. In patients with cerebral amyloid angiopathy (CAA), posterior pvWMHs and WMH multispots are associated with more severe WM rarefaction compared to NAWM [71]. Severe WM lesions are more common in patients with dementia, but the presence of amyloid in AD pathology and CAA is not directly associated with WM demyelination [102].

Similar findings were reported in VaD specimens. For example, WMHs are associated with areas of severe myelin pallor and irregularly shaped, fragmented myelin sheaths in individuals with VaD more strongly than in controls [59]. Interestingly, areas classified as NAWM on MRI also exhibit neuropathological abnormalities, characterized by an intermediate degree of myelin loss [59]. Similarly, hypertensive individuals exhibit greater WMH burden and severity than controls [85] and myelin loss, axonal damage, and microstructural alterations are present not only within WMHs but also in NAWM in individuals with hypertension. The authors hypothesized that the gradual increase in FLAIR signal intensity from NAWM toward hyperintense regions may reflect a progressive increase in the underlying burden of WM pathology. This hypothesis was supported by a lower polarized light imaging and LFB staining intensity associated with higher FLAIR signal intensity. Overall, hypertensive individuals also exhibit greater WMH burden than controls [85].

Regarding other types of NDDs, sporadic subcortical ischemic vascular dementia (i.e., type of VaD) shows milder perivascular and myelin changes than CADASIL (44–68 years old) and no temporal pole hyperintensities are noted in subcortical ischemic vascular dementia and significantly older controls (i.e.,

not age-matched: 75–90 years old). This supports disease-specific WMH mechanisms in CADASIL [86]. Finally, in ALS, WMHs are present in the corticospinal tract, reflecting axonal and myelin loss [77].

Axonal damage within WMHs

WMH lesions have been strongly associated with diffuse demyelination, astrocytic gliosis, axonal loss, and arteriolosclerosis [102]. Moderate-to-severe myelin pallor and axonal loss have been reported in the majority of cases with WMHs, regardless of diagnosis [96]. Compared with NAWM, WMHs exhibit significantly lower axonal density, greater demyelination, and increased SMI32 immunoreactivity, indicative of axonal dysfunction [74, 75]. Roseborough et al. similarly reported significant axonal loss in pvWMHs, reflected by reduced neurofilament (NF) field fraction, compared with NAWM in individuals with AD and CVD [57]. Axonal damage and demyelination are also observed in WMHs in individuals with vascular dementia, with these pathological alterations extending beyond the core of the lesions [97]. Furthermore, the largest WMH areas identified on MRI are associated with well-defined corresponding regions of reduced staining for both myelin and axonal markers. Conversely, regions exhibiting a thin rim of abnormality on MRI are associated with a correspondingly thin periventricular rim of reduced myelin and axonal staining [104].

Taken together, these findings suggest that demyelination and axonal loss occur concurrently within WMHs. However, these histopathological features may also reflect distinct underlying cellular mechanisms, which could explain the differential contributions of axonal and myelin pathology to MRI measures. For example, axonal density independently predicts fractional anisotropy [53] and FLAIR signal intensity [85], whereas T1 relaxation times are influenced by axonal density, myelin density, and microglial activation in both WMHs and NAWM [53]. Furthermore, NF staining predicts FLAIR signal intensity in NAWM but not in pvWMHs, suggesting that myelin loss may be the predominant contributor to the MRI signal within visible WMH lesions [57]. Consistent with this interpretation, another study demonstrated that disrupted axons are predominantly concentrated in patches within areas of more extensive myelin pallor. Conversely, numerous areas with relatively preserved myelin also exhibit axonal disruption, suggesting that axonal damage and demyelination may not always occur in parallel or be spatially coupled within WMHs [93].

Regional Patterns of Axonal damage

Comparing the pathological patterns of pvWMHs and dWMHs, Fazekas et al. showed that irregular pvWMHs are associated with pathological changes similar to those observed in confluent dWMHs, including myelin and fiber loss [1]. Subsequent studies using quantitative assessment of axonal fibers have provided further evidence of regional differences. Murray et al. reported a lower percentage of phosphorylated NF staining area (%pNF) in pvWMHs than in dWMHs [76]. Given that %pNF is associated with FLAIR signal intensity [76], and that FLAIR signal intensity exhibits a gradual increase from NAWM toward hyperintense regions [85], these findings may suggest that NAWM also exhibits some degree of axonal damage, potentially explaining the similar %pNF observed in dWMHs and NAWM [76]. Alternatively, the axons within dWMHs and NAWM may be relatively preserved compared with those in

pvWMHs. Supporting this possibility, another study found no significant difference in axonal degeneration between areas of posterior confluent WMHs, corresponding to dWMHs, and NAWM [71].

Axonal damage in AD and other NDDs

In AD, WMH severity is related to both axonal loss and demyelination, compared to WMHs in controls that are mainly related to demyelination [75]. Furthermore, in AD brains, parietal WMHs are linked to AD pathology (i.e., amyloid burden) as well as Wallerian degeneration rather than vascular pathology, while WMHs in control specimens show ischemic features [75]. Specimens with CADASIL also show axonal damage within WMHs, correlating with amyloid deposition [86].

Examining the combined effects of AD and CVD, Roseborough et al. found no additive effect of comorbid AD and CVD on axonal degeneration compared with CVD alone [57]. In contrast, WMHs and NAWM in individuals with hypertension are associated with increased axonal damage without evidence of greater demyelination, as hypertension is associated with higher pNF staining intensity [85]. Finally, ALS specimens exhibit axonal and neurofilament loss within WMHs of the lateral corticospinal tract, which are associated with decreased fractional anisotropy and increased mean diffusivity, T1, and T2 relaxation times compared with NAWM [77].

Neuroinflammation burden

Several early studies provide evidence of gliosis and neuroinflammation within WMH regions, including both periventricular and deep WMHs, compared with NAWM [1, 95, 101, 102, 104]. Subsequent studies have further supported the involvement of these processes and have identified WM vacuolation (i.e., spongiosis) within WMHs, which is associated with oxidative stress [76, 94, 103]. More recently, Desmarais et al. reported that the most frequent histological correlate of WMHs is moderate-to-severe gliosis, as assessed by GFAP staining. Furthermore, activated microglia and macrophage infiltration are observed in the majority of WMH cases, although generally at low levels [96].

WMH regions also exhibit increased vimentin immunoreactivity compared to NAWM, reflecting alterations in astrocytic intermediate filaments and potentially the BBB [79, 99]. Both studies also assessed Iba1 in WMHs and NAWM, but reported discrepant findings. Lahna et al. found no significant difference in Iba1 expression between WMHs and NAWM [99], whereas Silbert et al. reported significantly greater Iba1 expression in WMH regions [79]. This discrepancy may be partly explained by methodological and statistical power differences between the studies. Lahna et al. [99] used a semiquantitative scoring approach to assess Iba1 staining in 20 brains, whereas Silbert et al. quantified microglial expression using intensity-based image analysis in 51 individuals [79].

Another study supported that WMH regions exhibit greater neuroinflammation than NAWM and demonstrated alterations in the morphology of both astrocytes and microglia within WMHs [83]. Specifically, the authors reported 1) increased Iba1 staining intensity and microglial activation, 2) a more phagocytic microglial morphology, 3) shorter microglial ramifications, 4) a greater area occupied by GFAP-positive astrocytes, and 5) increased astrocytic activation, as assessed by morphological features

(Fig. 3C). Furthermore, moderate-to-severe WMH burden is associated with greater microglial activation and a larger microglial area, whereas astrogliosis and perivascular inflammation are not significantly associated with WMH burden [83].

Oxidative stress is another important feature of WMHs. Significant differences in the percentage of 8-OHdG-positive nuclei and γH2AX, both markers of oxidative DNA damage and DNA damage response, are reported between WM from controls and NAWM from patients with lesions elsewhere, as well as between WM from controls and WMHs [94]. Notably, markers of oxidative stress and DNA damage response are highest in NAWM from cases with lesions elsewhere, suggesting that oxidative stress may extend beyond areas of visible WMHs [94]. The same study also identified markers of cellular senescence, including SA-β-gal, within WMHs. Furthermore, Fernando et al. reported increased expression of hypoxia-inducible factors 1 and 2 (HIF-1 and HIF-2), key regulatory proteins involved in the cellular response to low oxygen availability, in WMHs compared to NAWM. This finding suggests an increased hypoxic or oxidative stress burden within WMHs [68].

Additional insights have emerged from studies examining associations between qMRI measures and neuroinflammatory markers. T1 relaxation time is independently associated with axonal density, myelin density, and microglial activation, as assessed by HLA-DR staining, whereas astrogliosis (GFAP score) is associated with fractional anisotropy [53]. Furthermore, lesions identified histologically by myelin attenuation but not detected on MRI (MRI-negative lesions) exhibit microglial and endothelial activation, suggesting that pathological changes may have clinical relevance even in the absence of a visible MRI abnormality [59].

Regional Differences in Neuroinflammation

Both pvWMHs and dWMHs exhibit increased microglial immunoreactivity compared to NAWM, with the greatest increase observed in pvWMHs [76, 80, 81]. The proportion of reactive astrocytes is also higher in pvWMHs than in dWMHs [76, 80]. Similarly, greater WM vacuolation is reported in both pvWMHs and dWMHs compared with NAWM, with vacuolation being particularly pronounced in pvWMHs relative to dWMHs [76].

Punctate, early confluent, and confluent dWMHs were associated with progressively greater severity of ischemic tissue damage, including myelin and fiber loss, gliosis, cavitation, and arteriolosclerosis. Irregular pvWMHs exhibited similar ischemic changes to those observed in confluent dWMHs, whereas caps and smooth halos were interpreted as predominantly non-ischemic changes associated with demyelination, subependymal gliosis, and ependymal disruption [1, 95, 103]. Finally, confluent WMHs were associated with higher densities of activated microglia and greater severity of clasmatodendrosis (i.e., swollen GFAP+ cell bodies with beaded processes), whereas multispots WMH were associated with WM rarefaction, as well as evidence of microglial activation and reactive astrocytosis [71].

Neuroinflammation in AD and other NDDs

Greater ventricular ependymal denudation and gliosis were observed in regions exhibiting loss of myelinated axons within the deep WM in AD brains [101]. Silbert et al. also reported greater disruption of water channels and more pronounced gliosis in posterior compared with anterior regions, potentially reflecting the involvement of posterior WMH as an early feature of AD [79]. Furthermore, Gouw et al. reported that all neuropathological measures differ between WMHs and NAWM; however, the difference in microglial activation is specific to AD [53]. Notably, a higher proportion of macrophages is observed in WMHs compared to NAWM among AD cases, whereas macrophage proportions were comparable between these tissue types in controls [53]. These findings may also explain the discrepant results reported by Silbert et al. and Lahna et al., both of which included individuals with AD and other forms of dementia [79, 99].

Compared to controls, cSVD cases had a significantly greater GFAP-immunoreactive area in periventricular WM, including both WMHs and NAWM [88]. This finding suggests an increased burden of astrogliosis throughout the periventricular WM in individuals with cSVD, consistent with their greater WMH burden [88]. Similarly, Chen et al. reported a 42-fold increase in the number of clasmatodendrocytes in post-stroke cases with dementia compared with post-stroke cases without dementia, as well as an approximately 11-fold increase in older compared with younger controls [67].

Furthermore, hypertension cases exhibited greater neuroinflammatory activity than controls in both WMHs and NAWM. Specifically, hypertension was associated with increased microglial activation and a more amoeboid microglial morphology, although microglial area was slightly reduced. Hypertension cases also exhibited greater astrogliosis than controls in both WMHs and NAWM, characterized by a larger GFAP-positive area and greater astrocytic activation [83].

Vascular pathology

Demyelination was shown as the primary underlying feature of WM lesions, but vascular integrity was the most reliable marker of WMHs [93]. Notably, vascular and BBB integrity were reduced within WMH regions compared to NAWM [93]. Vascular changes, including arteriosclerosis and dilated perivascular spaces (with the latter appearing secondarily) were prominent in different WMH patterns [95, 102]. Lesions detected by myelin attenuation alone (MRI-negative) still showed endothelial activation (including upregulation of ICAM-1/Collagen-IV ratio), suggesting clinical significance of the vascular pathology even in WMHs that were mildly visible through MRI [59]. Compared to NAWM, WMHs also showed a greater perivascular inflammation [83] and corresponded to about twofold greater vessel wall pathology as measured by stained area (Masson staining). WMHs also showed lower microvascular density, but greater BBB-related intensity and greater perivascular stain (5%) compared to NAWM [84].

Contradictory to these findings, McAleese et al. showed that in AD, WMH severity is associated with tau and amyloid burden but, less consistently, WM SVD [72]. Similarly, Scheltens et al. reported no significant correlations between WMHs and perivascular space width, CAA or other measured vascular variables [101]. They suggest that the main pathological substrates of WMH are loss of myelinated axons, gliosis, ventricular ependymal denudation, arterial adventitial fibrosis, but not arteriolosclerosis or CAA [101].

Furthermore, although present in half of the WMH regions, BBB integrity (using extravascular fibrinogen markers) is not related to WMHs [87].

Finally, Roseborough et al. investigated microvessel stenosis, perivascular spaces, and fibrinogen deposition in periventricular infarcts within pvWMHs. They found that periventricular venules and arterioles were significantly more stenotic in periventricular infarcts than in NAWM. In addition, perivascular spaces surrounding small arterioles and periventricular intraglial fibrinogen deposition were increased in periventricular infarcts compared with NAWM [78].

Venous collagenosis

Non-inflammatory thickening of the venous walls accompanied by increased collagen deposition, referred to as venous collagenosis, was reported as a characteristic feature of WMHs and was associated with WMH severity [56]. Moody and colleagues were among the first to systematically assess venous collagenosis using modified Masson's trichrome staining, in which collagen is stained blue, allowing for the assessment of venous wall thickness (Fig. 4). They demonstrated a strong association between the probability of severe leukoaraiosis and higher venous wall thickness scores [56]. Subsequent studies further supported the association between venous collagenosis and WMH burden. Specifically, venous collagenosis, characterized by reduced venous diameter (Fig. 4F, black arrow), increased venous collagen thickness (Fig. 4F, white arrow), and venular tortuosity (Fig. 4B), was identified as a significant predictor of greater pvWMH burden [69]. Moreover, venous collagenosis scores were positively correlated with WMH severity [98].

Regional Differences in Vascular pathology

pvWMHs were associated with gliosis, ependymal disruption and proliferation, vacuolated neuropil/myelin, and vascular sclerosis, and were generally considered age-related. dWMHs most commonly corresponded to vacuolated myelin around widened perivascular spaces and vascular changes [103]. More specifically, vascular features were not present in pvWMH rims, while caps were associated with arteriosclerosis [95]. Punctate dWMHs were associated with perivascular gliosis, arteriolar ectasia, and dilated perivascular spaces. Finally, WMH patches were associated with dilated perivascular spaces [95]. This corroborates findings of another study showing punctate WMHs that were associated with an increased size of perivascular spaces, multiple small infarcts, and amyloid deposition in arterioles [58]. However, these findings were contradictory to those of Fazekas et al. who reported that irregular pvWMH show similar ischemic changes to confluent dWMH, including cavitations, and arteriolosclerosis, while caps and smooth halo pvWMHs were interpreted as predominantly nonischemic changes [1].

Murray et al. investigated the density of small, medium and large vessels in pvWMHs compared to dWMHs and NAWM, and found that only small vessel density is associated with FLAIR signal intensity [76]. Small vessel density is reduced in WMHs (either periventricular or deep) compared to NAWM, but it does not differ between pvWMHs compared to dWMHs, suggesting that vascular pathology is similar

regardless of the WMH location [76]. However, other findings suggest that pvWMH volume is associated with arteriosclerosis, while dWMHs are associated with cortical microinfarcts and cerebral hemorrhages [1, 91]. They also reported that the vessel wall thickness is not associated with WMHs [91].

Furthermore, frontal WMH severity was associated with arteriolosclerosis in both AD and controls [74]. They suggested that frontal WMHs in AD likely reflect both SVD-related and AD-associated degenerative mechanisms [74]. In another study, posterior confluent WMHs were associated with arteriolosclerosis severity in brains with CAA [71]. They did not observe differences in dWMH perivascular space area between different lobes [71]. Furthermore, in brains with AD, posterior compared with anterior regions showed greater water channel disruption and gliosis (as measured by aquaporin markers and vimentin for the BBB integrity), which were decreased in WMHs compared to NAWM, possibly reflecting posterior WMH as early AD feature [79].

Another study found that voxel-wise FLAIR signals positively correlated with vessel wall area, microvasculature intensity, and negatively with microvascular density [84]. They also showed that Masson's Trichrome area was larger in the core of WMH, represented by the highest FLAIR intensity, compared with adjacent WMH segments. These findings suggest that vessel wall pathology shows some gradient within established WMH, indicating that these processes may already be present in NAWM or occur at a finer scale than captured by the segments [84]. This corroborates the conclusion that proximal NAWM show similar but milder vascular abnormalities that diminish with distance from WMH [79].

Vascular pathology in AD and other NDDs

Moody et al. showed that vessel density (as measured by alkaline-phosphatase staining) is significantly decreased in WMHs compared to NAWM. However, there is no significant vessel density decline with age in WMHs. While mean vessel density in NAWM of cases with leukoaraiosis is less than that of cases without leukoaraiosis, the difference is not significant [90]. However, when these same data were plotted in relation to age, the slopes describing the age-associated vascular density in cases with leukoaraiosis significantly differed from age-matched healthy cases. In healthy cases, vessel density was reduced by approximately 28.8% per decade (between 57 and 87 years old), while vessel density of NAWM of cases with leukoaraiosis elsewhere decreased by 47% [90].

Scheltens et al. showed that WMHs of AD specimens show vascular wall changes, but not classic arteriolosclerosis. They found no significant AD-control difference in perivascular spaces, while arterial adventitial fibrosis and external collagenous layer thickness in dWMHs arteries were greater in AD [101]. These findings suggest that WMHs in AD and control individuals without cerebrovascular risk factors likely reflect accelerated aging and not distinct AD-specific small-vessel disease.

Similarly, Desmarais et al. reported that vascular pathology in the form of venous collagenosis is occasionally present in WMHs of AD patients, but that none of their cases show arteriolosclerosis, infarction, or perivascular hemosiderin (microbleeds) [96]. Likewise, Roseborough et al. showed no

association between AD diagnosis (10/20) and vascular, fibrinogen, or microglial measures [78]. Furthermore, McAleese et al. showed that parietal WMHs of AD patients are linked to cortical AD pathology and Wallerian degeneration rather than SVD, while WMH from controls show ischemic features [75]. The same group then demonstrated that control cases have more WMH fibrinogen in high SVD, which is related to sclerosis index, while this is not the case in AD [73].

On the contrary, Van Swieten et al. reported that brains with moderate-to-severe demyelination had more arteriolosclerosis [102]. Similarly, Keith et al. reported that arteriolosclerosis was more frequently present (66.7%) in WMHs in AD cases compared to non-AD [98]. Furthermore, venous collagenosis scores increased, collagenosis severity of small and medium caliber periventricular veins increased, and the large vein stenosis was also significantly greater only when WMH burden was high, suggestive of an association between WMH and vascular pathology severity [98]. They also reported that in the AD group, WMH scores significantly correlated with large veins stenosis, while WMH scores of the non-AD group significantly correlated with venous collagenosis, reflecting that overall, the strongest predictor of WMH scores was the large veins stenosis [98]. This is consistent with findings from a study conducted in familial AD that reported substantial SVD pathology despite relatively mild WMHs on MRI [70]. Their findings included enlarged perivascular spaces, arteriosclerosis, fibrinogen-positive leaking vessels, reduced PDGFRβ-positive perivascular coverage, and reduced AQP4-positive astrocytic end-feet [70].

WMHs were also associated with vascular pathology across different forms of vascular dementia. Fernando et al. found that while the internal diameter of the blood vessels is not reduced in WMHs, their wall thickness within WMHs was significantly increased compared with NAWM, although this finding was not related to the presence of dementia [68]. Furthermore, perivascular spaces were enlarged within WMHs and were slightly greater in cases with dementia. They also found no significant variation in the density of the capillary network between dementia and non-dementia groups. Finally, a higher CAA load, both in parenchymal and leptomeningeal vessels, was associated with elevated HIF-1 expression (oxidative stress) in dWMHs compared with NAWM [68].

In brains of cases with hypertension, both WMH and NAWM regions showed higher levels of perivascular inflammation than controls [83]. Hypertension was also associated with lower vessel stenosis index, endothelial and metabolic response, vascular remodeling, BBB damage, and neuroinflammation in NAWM and WMH [84]. Finally, temporal pole WMHs strongly corresponded to enlarged perivascular spaces in CADASIL cases, which had a greater burden in CADASIL compared to controls. Furthermore, these brains showed marked vessel wall pathology [86]. Finally, vascular pathology was examined in any of the ALS cases.

Discussion

This review assessed 45 research articles to characterize the histopathological correlates of WMHs. Across different studies, WMHs were characterized by myelin loss (including spongiosis), axonal

rarefaction, edema, perivascular space dilation, gliosis, arteriolosclerosis, and venous collagenosis, all of which are indicative of underlying WM pathology [53–55, 57, 69].

Among the 29 studies that assessed demyelination, 22 (75.6%) specifically reported myelin pallor or myelin loss in WMHs compared to NAWM [1, 44, 53, 56–59, 74–77, 80, 85, 91, 95–99, 101, 102, 104]. Studies directly comparing severity of demyelination also found increased demyelination in pvWMHs compared to dWMHs [1, 76, 80, 95, 104]. Sixteen studies had assessed axonal damage, in which 14 (87.5%) reported neurofilament loss, axonal degeneration, or reduced axon density [1, 53, 57, 58, 74–77, 85, 86, 96, 97, 102, 104] while two studies (12.5%) showed no difference in axonal damage [71, 73]. Studies directly comparing pvWMHs and dWMHs also showed that axonal damage is higher in pvWMHs compared to dWMHs [1, 76, 85].

Out of the 22 studies that assessed neuroinflammation, sixteen (72.7%) reported an increase in gliosis [1, 53, 56, 67, 76, 79, 83, 88, 94–96, 99, 101–104] especially in pvWMHs, and this was also associated with hypertension [83]. Furthermore, seven studies reported that WMHs are related to edema corresponding to vacuolation (i.e., spongiosis) [56, 58, 76, 95, 103] or perivascular ischemia [83, 84]. Thirteen studies assessed microglial activation as a neuroinflammation marker, where twelve studies (92.3%) pointed to an increase of microglial activation in WMHs compared to NAWM [53, 59, 68, 71, 76–81, 83, 94]. One study found no significant difference in microglial activation in WMH and NAWM [99]. Microglial activation seemed to be more pronounced in pvWMHs compared to dWMHs in some studies [76, 81], while another study reported the opposite [80]. Their contradictory findings might be due to differences in covariates and specimens' clinical diagnosis, since microglial activation has been identified as a specific underlying feature of WMH in AD [53].

Associations between WMH burden and postmortem markers of neuroaxonal and astroglial injury are also supported by in vivo findings, as higher levels of plasma GFAP and NF were associated with greater global WMH burden in healthy aging and across different clinical populations. Both GFAP and NF were positively associated with baseline global WMH burden in cognitively unimpaired, MCI, and AD participants [105, 106], as well as with WMH progression over time across AD/MCI, Parkinson's disease, frontotemporal dementia, CVD, and healthy groups [107, 108]. GFAP was also associated with baseline WMH burden specifically among amyloid-positive cognitively healthy and MCI participants, suggesting that this relationship may be influenced by underlying amyloid pathology [109].

Among the 31 studies that assessed vascular pathology, 11 assessed artery health, showing that WMHs have increased arterioles density, wall thickness (i.e., stenosis) and arteriosclerosis [1, 58, 70, 71, 74, 78, 91, 95, 98, 101, 102]. On the contrary, two studies showed no association between WMHs and arteriolosclerosis [96, 101]. Studies also reported enlarged perivascular spaces (N = 11) in WMHs compared to NAWM [44, 58, 70, 71, 83, 84, 95, 101–104]. Only three other studies assessed BBB integrity and showed an increase of BBB damage in WMHs that corresponded to fibrinogen deposition [80, 84, 93]. Finally, venous collagenosis was the last feature corresponding to vascular pathology that was considered in this review. Five studies reported thickening of venous vessel walls within WMHs, and

found that greater venous disease was associated with greater WMH burden, especially in pvWMHs and AD [56, 69, 96, 98, 101].

Relatively few studies had comprehensively investigated the neuropathological features underlying WMHs while accounting for sex, different NDDs, or anatomical brain regions. One study focusing on vascular pathology reported that female sex and older age at death were strong predictors of greater pvWMH burden in AD brains [69]. However, it remains unclear whether these associations are specific to AD or extend to other NDDs, and whether similar relationships are observed across different WMH locations.

WMH patterns and distribution

pvWMHs consistently showed greater reductions in myelin immunoreactivity, axonal density and neurofilament loss, more pronounced astrogliosis and microglial activation, and greater neuropil vacuolation than dWMHs [76], which corresponded more to vascular pathology. While pvWMHs and dWMHs may present different underlying histopathology features overall, they can occur in proximity and share neighboring NAWM. Given that this surrounding NAWM may itself not be neuropathologically normal, this raises an important question regarding the gradient or relationship linking pvWMH and dWMH through this normal-appearing tissue. It remains unclear how the perilesional gradient affects the surrounding NAWM and whether regions considered normal based on FLAIR or T2w MRI are truly neuropathologically normal.

Perilesional penumbra is identified as a critical transition zone between WMHs and NAWM [12, 40, 110, 111]. Indeed, tissue surrounding WMHs exhibits a gradient of microstructural rarefaction, extracellular fluid expansion, perfusion deficits, and reduced vascular reactivity that extends beyond the visible lesion boundaries [112]. This is consistent with studies demonstrating reduced cerebral blood flow and cerebrovascular reactivity, as well as increased BBB permeability, in NAWM of older individuals with WMHs [12, 110]. Similarly, pathological changes can extend into the surrounding NAWM, particularly within the immediate perilesional tissue, indicating that WMH pathology represents a diffuse process affecting a substantial proportion of the WM. Consequently, the WMHs visible on conventional MRI may represent only the “tip of the iceberg” of the underlying pathological process [111].

Among the studies that were assessed within our review, only three adjusted their analyses according to the distance between dWM and pvWM [79, 84, 85]. They reported that proximal NAWM showed similar but milder demyelination, neuroinflammation markers and vascular pathology to WMH regions, which diminished with distance from WMH [79]. Furthermore, Sole-Guardia et al. showed a gradient of pathology across FLAIR-intensity segments, where a higher FLAIR-intensity segment showed lower LFB myelin and NF intensity [85]. Vascular pathology also showed some gradient within established WMH, but BBB damage and inflammation did not show a gradual NAWM-to-WMH gradient [84]. Taken together, these findings highlight the importance of considering WMH pathology as a spatial gradient rather than as a binary distinction between WMH and NAWM. Future histopathological studies should therefore

investigate the distribution of demyelination, axonal damage, neuroinflammation, and vascular pathology as a function of distance from the WMH core into the surrounding NAWM. Such an approach may provide a more comprehensive characterization of the pathological continuum underlying WMHs and help determine whether MRI-defined NAWM can truly be considered pathologically normal.

Another important consideration when examining WMH distribution is their anatomical location according to lobar regions, as the regional distribution of WMHs may be relevant to their clinical and pathological significance. Anterior-to-posterior WMH distribution was assessed in only 18 of the 45 studies included in our review [53, 56, 67, 69–72, 77, 79, 89, 92, 93, 97, 99–103]. However, only four of these studies directly compared the histopathological features of WMHs between frontal and occipital regions [71, 79, 99, 102]. However, as most studies include multiple regional WMH blocks to increase sample size (e.g., 7 brains, 29 blocks [95], 7 brains, 69 blocks [104], 4 brains, 81 blocks [76]), it remains unclear whether WMHs in frontal and occipital regions differ in their underlying histopathological features. Anatomical location should therefore be considered in statistical analyses of WMH pathology in future studies.

Regional molecular changes may provide additional insights into region specific WMH differences. Malla et al. investigated molecular upregulation and downregulation within WMH regions in AD compared with controls [89]. In frontal WMHs, AD cases showed upregulation of pathways related to DNA damage response, tube morphogenesis, and regulation of hippo signaling (i.e., cell proliferation and apoptosis), together with downregulation of trans-synaptic signaling, axon guidance, cellular homeostasis, and oxidative phosphorylation [89]. These findings suggest that frontal WMHs in AD may involve alterations in DNA damage responses, vascular processes, synaptic function, and cellular metabolism, consistent with histopathological evidence of axonal damage in AD WMHs [75]. In contrast, occipital WMHs showed upregulation of epithelial cell differentiation and tissue morphogenesis pathways, together with downregulation of cell-cycle regulation and responses to reactive oxygen species [89]. These molecular alterations may reflect the involvement of vascular and inflammatory processes in posterior WMHs. This interpretation is consistent with the findings of Desmarais et al., who reported greater occipital WMH burden in AD, and Silbert et al., who demonstrated greater water channel disruption and gliosis in posterior compared with anterior WM regions [79, 96]. Together, these findings raise the possibility that posterior WMHs may represent an early or particularly relevant pathological feature of AD.

Correlation between qMRI and histology assessment in WMHs

While qMRI could be used as in vivo proxies of WMH pathology, their biological specificity and sensitivity need to be determined in the context of WMHs. Only three included studies correlated qMRI markers to histopathological markers in WMHs. In ALS, Pallebage-Gamarallage et al. reported a significant decrease in average fractional anisotropy value and a significant increase in average mean diffusivity, T1 and T2 values in WMHs compared to NAWM [77]. Furthermore, where qT1 is sensitive to axonal density, myelin density and microglial activation, fractional anisotropy might be more closely associated with axonal

density [53]. Therefore, since a reduction in fractional anisotropy is observed in WMHs, it was expected that axonal damage would be one of the main pathological features observed in WMHs, as shown in multiple studies [57, 74, 75, 86, 96, 97, 102, 104]. These findings are consistent with other studies assessing qMRI, where WMHs exhibited higher mean diffusivity and lower fractional anisotropy, magnetization transfer ratio, myelin water fraction and T1/T2 ratios compared with NAWM, suggestive of myelin loss and axonal degeneration [64, 112].

Given that qT2* has been identified as one of the strongest predictors of WM damage [4], and that qT2* is associated with both myelin loss [113] and iron accumulation [114, 115], we anticipated that iron deposition would represent an important pathological feature of WMHs [116]. Surprisingly, none of the included studies assessed ferritin immunoreactivity, and only one study used Perls' Prussian blue staining to evaluate iron deposition within the corpus callosum, but not within WMH regions [97]. Therefore, despite the potential relevance of iron accumulation to qMRI measures and WMH pathology, its contribution to the histopathological features of WMHs remains largely unexplored. Further studies are warranted to elucidate the potential impact of hemosiderin (i.e., pathological iron commonly found in microbleeds) compared to ferritin (i.e., iron stockage form, also present within macrophages) [117–119] in WMHs. Preliminary results of our team suggest a relationship between WMHs and hemosiderin accumulation along with a reduced ferritin density compared to NAWM (Fig. 5).

Association of WMHs with neurodegeneration

Among the 16 studies that focused on AD, 9 directly reported that histopathology features of WMHs are more pronounced in AD compared to healthy controls [53, 72–75, 89, 98, 101, 104], while one found so significant difference between AD and controls [96]. Associations between WMH severity and AD pathology (amyloid and tau) mirror in vivo findings whereby increased baseline levels of both amyloid and tau (measured based on positron emission tomography, cerebrospinal fluid, or plasma markers) are associated with both greater baseline and faster progression of WMHs [39, 120–123]. These associations might also show distinct regional patterns. Kamal et al. reported associations between baseline amyloid burden and WMH progression in the frontal and parietal lobes, whereas greater baseline tau burden was associated with increased WMH progression only in the parietal lobe [122]. Lower cerebrospinal fluid Aβ and tau levels have also been associated with posterior [124], parietal, and temporal WMHs [125].

The relationship between WMHs and vascular pathology in AD remains inconsistent. Earlier studies reported no significant association between WMHs and CAA [101, 102]. McAleese et al. subsequently reported that both CAA and WMH burden were greater in AD than in controls. However, CAA was not associated with increased fibrinogen deposition in WMHs compared with NAWM, and neither CAA nor SVD emerged as major correlates of parietal WMH burden [73, 75]. Conversely, Desmarais et al. reported that AD cases with concomitant CAA had greater parietal WMH burden than AD cases without CAA, suggesting that CAA may contribute to WMH pathology in some AD cases [96].

Neuroinflammation may represent another important disease-specific component of WMH pathology in AD. AD cases show greater microglial activation than controls [53], as well as a higher proportion of clasmatodendrocytes, which was also associated with lower cognitive performance [67]. In contrast, AD cases have not consistently shown greater vascular pathology than controls [98]. These findings suggest that neuroinflammatory mechanisms may contribute substantially to WMH pathology in AD, particularly in posterior regions where WMH burden appears to be more pronounced [96]. A similar relationship between MRI abnormalities and neuroinflammation has been reported in ALS. Pallebage-Gamarallage et al. demonstrated that qT2* and QSM hyperintensity in ALS were primarily associated with CD68-positive microglial activation suggesting that inflammatory processes may also contribute to MRI-detectable white matter abnormalities in other NDDs [77].

Overall, our findings suggest that WMHs represent a heterogeneous pathological entity across NDDs. Although WMH burden is not consistently associated with a single pathological mechanism in AD, disease-specific differences in regional distribution, neuroinflammation, vascular pathology, and AD-related proteinopathy may contribute to their development and clinical significance. The substantially greater WMH burden observed in CADASIL further highlights the importance of vascular mechanisms, while the variable findings across AD and other NDDs emphasize the need to consider both disease diagnosis and anatomical location when interpreting the neuropathological substrates of WMHs.

Future directions

Certain limitations warrant acknowledgment. The limited number of available studies and their heterogeneity in terms of methodology, region of interest, and NDD conditions included, restricted our work to a systematic review rather than allowing for a meta-analysis. This limitation reflects the current state of the literature, further emphasizing the need for future investigations of WMH pathological substrates across different brain regions and NDDs using gold-standard histopathology. Standardized definitions of WMH location and severity, harmonized histopathological protocols, and consistent reporting of clinical, imaging, and tissue-level variables will also be important to facilitate comparisons across studies and enable future quantitative synthesis and meta-analyses. Future studies should also prioritize systematic validation of qMRI biomarkers against histopathological measures within the same tissue regions, with multimodal qMRI measures evaluated against specific pathological substrates rather than WMH status alone.

Studies with larger sample sizes and more direct comparisons across different NDDs and sexes are needed to better characterize sex- and disease-specific patterns of WMH pathology, especially in Parkinson's disease, Lewy body dementia and ALS, within which WMHs remain underexplored. In addition, statistical analyses should account for the anatomical location of WMHs, including anterior versus posterior or lobar distinctions, pvWMHs versus dWMHs (also separating juxtacortical and scWMHs where possible), as well as their spatial gradient and distance from surrounding NAWM. For example, the distance from the WMH core could be incorporated as a covariate or examined using concentric perilesional rings to characterize progressive pathological changes from the lesion core toward NAWM. This approach would help determine whether MRI-defined NAWM is truly

neuropathologically normal and identify the spatial extent of pathological changes beyond the visible WMH boundaries.

Further investigation is also warranted to better characterize axonal degeneration and iron accumulation as potential predictors or outcomes of WMHs. Axonal pathology could be assessed using complementary approaches, including neurofilament and SMI immunohistochemistry and Bielschowsky silver staining. Similarly, iron accumulation could be investigated using both ferritin immunohistochemistry and Perls' Prussian blue staining, which would allow for the assessment of ferritin- and hemosiderin-associated iron deposition, respectively. Multimodal histopathological approaches incorporating markers of myelin, axonal integrity, astroglial and microglial responses, vascular pathology, blood–brain barrier disruption, and iron accumulation would provide a more comprehensive characterization of the heterogeneous pathological processes underlying WMHs.

In brief, larger, standardized, multi-stain investigations of the histopathological features of WMHs across sexes, anatomical regions, and NDDs are essential to better understand the underlying mechanisms of these lesions and ultimately facilitate the development of reliable biomarkers capable of distinguishing the heterogeneous pathologies associated with WMHs across different neurodegenerative disorders.

Sources of funding

EMF receives postdoctoral fellowships from the Fonds de Recherche du Québec - Santé (FRQS) (https://doi.org/10.69777/361834), the Alzheimer’s Society Research Program (ASRP) (Postdoctoral, Biomedical: #0000000173), and BrainHealth Care (BHCare) Canada. AM receives doctoral scholarships from the FRQS (https://doi.org/10.69777/344731) and the Vascular training (VAST) Platform. OP is supported by the ASRP and FRQS. KC receives a Canada Graduate Research Scholarship, Master's, from the Canadian Institutes of Health Research (CIHR) and a doctoral scholarship from VAST. FK receives a postdoctoral fellowship from FRQS. ZA is supported by the NSERC Vanier scholarship. ABR reports receiving a doctoral scholarship from FRQS (https://doi.org/10.69777/362882). RM receives a doctoral scholarship from the FRQS (https://doi.org/10.69777/350961). SR receives doctoral scholarships from the VAST, BHCare, and FRQS (https://doi.org/10.69777/2007562). NT receives funding from the Integrated Program in Neuroscience at McGill University. YZ reports receiving research funding from the FRQS (https://doi.org/10.69777/320107), Natural Sciences and Engineering Research (NSERC), and CIHR. MD reports receiving research funding from the CIHR (191303, 198104, and 213169), NSERC discovery grant (RGPIN-2023-04038), FRQS (https://doi.org/10.69777/330750), ASRP, and Tier-2 Canada Research Chair in Vascular and Neurodegenerative Disorders of Aging.

Declarations

Disclosures

The authors report no competing interests.

References

1. Fazekas, F., et al., *Pathologic correlates of incidental MRI white matter signal hyperintensities.* Neurology, 1993. **43**(9): p. 1683-9.
2. Alber, J., et al., *White matter hyperintensities in vascular contributions to cognitive impairment and dementia (VCID): Knowledge gaps and opportunities.* Alzheimers Dement (N Y), 2019. **5**: p. 107-117.
3. Boutzoukas, E.M., et al., *Frontal White Matter Hyperintensities and Executive Functioning Performance in Older Adults.* Front Aging Neurosci, 2021. **13**: p. 672535.
4. Parent, O., et al., *Assessment of white matter hyperintensity severity using multimodal magnetic resonance imaging.* Brain Commun, 2023. **5**(6): p. fcad279.
5. Kamal, F., et al., *Intersecting vulnerabilities: race, depression, and white matter hypointensity burden in aging.* Alzheimers Dement (Amst), 2026. **18**(1): p. e70252.
6. Marquine, M.J., et al., *Differential patterns of cognitive decline in anterior and posterior white matter hyperintensity progression.* Stroke, 2010. **41**(9): p. 1946-50.
7. Parent, O., et al., *Characterizing spatiotemporal white matter hyperintensity pathophysiology in vivo to disentangle vascular and neurodegenerative contributions.* Nat Commun, 2026. **17**(1).
8. Dadar, M., et al., *White matter hyperintensity distribution differences in aging and neurodegenerative disease cohorts.* Neuroimage Clin, 2022. **36**: p. 103204.
9. Kamal, F., et al., *White Matter Hyperintensity Trajectories in Patients With Progressive and Stable Mild Cognitive Impairment.* Neurology, 2023. **101**(8): p. e815-e824.
10. Kamal, F., et al., *Topographical differences in white matter hyperintensity burden and cognition in aging, MCI, and AD.* Geroscience, 2023. **45**(1): p. 1-16.
11. Bailey, E.L., et al., *Pathology of lacunar ischemic stroke in humans--a systematic review.* Brain Pathol, 2012. **22**(5): p. 583-91.
12. Uh, J., et al., *In vivo vascular hallmarks of diffuse leukoaraiosis.* J Magn Reson Imaging, 2010. **32**(1): p. 184-90.
13. Wardlaw, J.M., et al., *Neuroimaging standards for research into small vessel disease and its contribution to ageing and neurodegeneration.* Lancet Neurol, 2013. **12**(8): p. 822-38.
14. de Leeuw, F.E., et al., *Prevalence of cerebral white matter lesions in elderly people: a population based magnetic resonance imaging study. The Rotterdam Scan Study.* J Neurol Neurosurg Psychiatry, 2001. **70**(1): p. 9-14.
15. Garnier-Crussard, A., et al., *White matter hyperintensities in Alzheimer's disease in the era of anti-amyloid therapies.* Alzheimers Dement (Amst), 2026. **18**(2): p. e70349.
16. Yang, K., et al., *White matter changes in Parkinson's disease.* NPJ Parkinsons Dis, 2023. **9**(1): p. 150.
17. Chen, Z.C., et al., *The vascular risk factors and vascular neuropathology in subjects with autopsy-confirmed dementia with Lewy bodies.* Int J Geriatr Psychiatry, 2022. **37**(3).

18. Singh-Reilly, N., et al., *White matter hyperintensities in dementia with lewy bodies and posterior cortical atrophy.* Neurobiol Aging, 2025. **150**: p. 44-52.
19. Dadar, M., et al., *White matter hyperintensities are associated with grey matter atrophy and cognitive decline in Alzheimer's disease and frontotemporal dementia.* Neurobiol Aging, 2022. **111**: p. 54-63.
20. Chadwick, K., et al., *White matter hyperintensities as biomarkers in ALS: link to disease severity, progression, survival, and medication response.* medRxiv, 2026: p. 2026.04.28.26351973.
21. Luo, W., et al., *White matter hyperintensities and the risk of vascular dementia: a systematic review and meta-analysis.* PeerJ, 2025. **13**: p. e19460.
22. Wen, W., et al., *White matter hyperintensities in the forties: their prevalence and topography in an epidemiological sample aged 44-48.* Hum Brain Mapp, 2009. **30**(4): p. 1155-67.
23. Wen, W. and P. Sachdev, *The topography of white matter hyperintensities on brain MRI in healthy 60- to 64-year-old individuals.* Neuroimage, 2004. **22**(1): p. 144-54.
24. Roseborough, A.D., et al., *White matter hyperintensities and longitudinal cognitive decline in cognitively normal populations and across diagnostic categories: A meta-analysis, systematic review, and recommendations for future study harmonization.* Alzheimers Dement, 2023. **19**(1): p. 194-207.
25. Lam, B.Y.K., et al., *High burden of cerebral white matter lesion in 9 Asian cities.* Sci Rep, 2021. **11**(1): p. 11587.
26. Beyer, F., et al., *White matter hyperintensity spatial patterns: Risk factors and clinical correlates.* Alzheimers Dement, 2025. **21**(4): p. e70053.
27. Lin, K., et al., *Risk factors and cognitive correlates of white matter hyperintensities in ethnically diverse populations without dementia: The COSMIC consortium.* Alzheimers Dement (Amst), 2024. **16**(1): p. e12567.
28. Raeesi, S., C. Morrison, and M. Dadar, *Education is associated with vascular risk factors and cerebrovascular disease burden in racially diverse individuals on the Alzheimer's disease spectrum.* Alzheimers Dement, 2025. **23;21**.
29. Sachdev, P., X. Chen, and W. Wen, *White matter hyperintensities in mid-adult life.* Curr Opin Psychiatry, 2008. **21**(3): p. 268-74.
30. Zheng, K., et al., *Analysis of Risk Factors for White Matter Hyperintensity in Older Adults without Stroke.* Brain Sci, 2023. **13**(5).
31. Debette, S., et al., *Clinical Significance of Magnetic Resonance Imaging Markers of Vascular Brain Injury: A Systematic Review and Meta-analysis.* JAMA Neurol, 2019. **76**(1): p. 81-94.
32. Clancy, U., et al., *Neuropsychiatric symptoms associated with cerebral small vessel disease: a systematic review and meta-analysis.* Lancet Psychiatry, 2021. **8**(3): p. 225-236.
33. Debette, S. and H.S. Markus, *The clinical importance of white matter hyperintensities on brain magnetic resonance imaging: systematic review and meta-analysis.* Bmj, 2010. **341**: p. c3666.
34. Herrmann, L.L., M. Le Masurier, and K.P. Ebmeier, *White matter hyperintensities in late life depression: a systematic review.* J Neurol Neurosurg Psychiatry, 2008. **79**(6): p. 619-24.

35. Tullberg, M., et al., *White matter lesions impair frontal lobe function regardless of their location.* Neurology, 2004. **63**(2): p. 246-53.
36. van Dijk, E.J., et al., *Progression of cerebral small vessel disease in relation to risk factors and cognitive consequences: Rotterdam Scan study.* Stroke, 2008. **39**(10): p. 2712-9.
37. Anor, C.J., et al., *The Longitudinal Assessment of Neuropsychiatric Symptoms in Mild Cognitive Impairment and Alzheimer's Disease and Their Association With White Matter Hyperintensities in the National Alzheimer's Coordinating Center's Uniform Data Set.* Biol Psychiatry Cogn Neurosci Neuroimaging, 2021. **6**(1): p. 70-78.
38. Misquitta, K., et al., *White matter hyperintensities and neuropsychiatric symptoms in mild cognitive impairment and Alzheimer's disease.* Neuroimage Clin, 2020. **28**: p. 102367.
39. Dadar, M., et al., *Cognitive and motor correlates of grey and white matter pathology in Parkinson's disease.* Neuroimage Clin, 2020. **27**: p. 102353.
40. Chung, S.J., et al., *White matter hyperintensities as a predictor of freezing of gait in Parkinson's disease.* Parkinsonism Relat Disord, 2019. **66**: p. 105-109.
41. Dadar, M., et al., *White matter hyperintensities mediate the impact of amyloid ß on future freezing of gait in Parkinson's disease.* Parkinsonism Relat Disord, 2021. **85**: p. 95-101.
42. Zou, X., et al., *White matter hyperintensities burden in the frontal regions is positively correlated to the freezing of gait in Parkinson's disease.* Front Aging Neurosci, 2023. **15**: p. 1156648.
43. Gebeily, S., et al., *Cerebral white matter hyperintensities (WMH): an analysis of cerebrovascular risk factors in Lebanon.* Int J Neurosci, 2014. **124**(11): p. 799-805.
44. Haller, S., et al., *Do brain T2/FLAIR white matter hyperintensities correspond to myelin loss in normal aging? A radiologic-neuropathologic correlation study.* Acta Neuropathol Commun, 2013. **1**: p. 14.
45. Kim, K.W., J.R. MacFall, and M.E. Payne, *Classification of white matter lesions on magnetic resonance imaging in elderly persons.* Biol Psychiatry, 2008. **64**(4): p. 273-80.
46. Grambaite, R., et al., *Executive dysfunction in mild cognitive impairment is associated with changes in frontal and cingulate white matter tracts.* J Alzheimers Dis, 2011. **27**(2): p. 453-62.
47. Smith, E.E., et al., *Correlations between MRI white matter lesion location and executive function and episodic memory.* Neurology, 2011. **76**(17): p. 1492-9.
48. Leritz, E.C., et al., *Associations between T1 white matter lesion volume and regional white matter microstructure in aging.* Hum Brain Mapp, 2014. **35**(3): p. 1085-100.
49. Maillard, P., et al., *White matter hyperintensity penumbra.* Stroke, 2011. **42**(7): p. 1917-22.
50. Maillard, P., et al., *White matter hyperintensities and their penumbra lie along a continuum of injury in the aging brain.* Stroke, 2014. **45**(6): p. 1721-6.
51. Black, S., F. Gao, and J. Bilbao, *Understanding white matter disease: imaging-pathological correlations in vascular cognitive impairment.* Stroke, 2009. **40**(3 Suppl): p. S48-52.
52. Gouw, A.A., et al., *Heterogeneity of small vessel disease: a systematic review of MRI and histopathology correlations.* J Neurol Neurosurg Psychiatry, 2011. **82**(2): p. 126-35.

53. Gouw, A.A., et al., *Heterogeneity of white matter hyperintensities in Alzheimer's disease: post-mortem quantitative MRI and neuropathology.* Brain, 2008. **131**(Pt 12): p. 3286-98.
54. Hachinski, V.C., P. Potter, and H. Merskey, *Leuko-araiosis: an ancient term for a new problem.* Can J Neurol Sci, 1986. **13**(4 Suppl): p. 533-4.
55. Humphreys, C.A., C. Smith, and J.M. Wardlaw, *Correlations in post-mortem imaging-histopathology studies of sporadic human cerebral small vessel disease: A systematic review.* Neuropathol Appl Neurobiol, 2021. **47**(7): p. 910-930.
56. Moody, D.M., et al., *Periventricular venous collagenosis: association with leukoaraiosis.* Radiology, 1995. **194**(2): p. 469-76.
57. Roseborough, A.D., et al., *Post-mortem 7 Tesla MRI detection of white matter hyperintensities: A multidisciplinary voxel-wise comparison of imaging and histological correlates.* Neuroimage Clin, 2020. **27**: p. 102340.
58. Munoz, D.G., et al., *Pathologic correlates of increased signals of the centrum ovale on magnetic resonance imaging.* Arch Neurol, 1993. **50**(5): p. 492-7.
59. Fernando, M.S., et al., *Comparison of the pathology of cerebral white matter with post-mortem magnetic resonance imaging (MRI) in the elderly brain.* Neuropathol Appl Neurobiol, 2004. **30**(4): p. 385-95.
60. Meng, F., Y. Yang, and G. Jin, *Research Progress on MRI for White Matter Hyperintensity of Presumed Vascular Origin and Cognitive Impairment.* Front Neurol, 2022. **13**: p. 865920.
61. Bastin, M.E., et al., *Diffusion tensor and magnetization transfer MRI measurements of periventricular white matter hyperintensities in old age.* Neurobiol Aging, 2009. **30**(1): p. 125-36.
62. Fazekas, F., et al., *MTI of white matter hyperintensities.* Brain, 2005. **128**(Pt 12): p. 2926-32.
63. Garnier-Crussard, A., et al., *Heterogeneity of white matter hyperintensities in Alzheimer's disease captured by multimodal neuroimaging.* Sci Rep, 2025. **15**(1): p. 38433.
64. Maniega, S.M., et al., *White matter hyperintensities and normal-appearing white matter integrity in the aging brain.* Neurobiol Aging, 2015. **36**(2): p. 909-18.
65. O'Sullivan, M., et al., *Diffusion tensor MRI correlates with executive dysfunction in patients with ischaemic leukoaraiosis.* J Neurol Neurosurg Psychiatry, 2004. **75**(3): p. 441-7.
66. Frigon, E.M., et al., *Effects of prolonged fixation on vascular biomarkers in postmortem human brains.* J Cereb Blood Flow Metab, 2026: p. 271678x261461536.
67. Chen, A., et al., *Frontal white matter hyperintensities, clasmatodendrosis and gliovascular abnormalities in ageing and post-stroke dementia.* Brain, 2016. **139**(Pt 1): p. 242-58.
68. Fernando, M.S., et al., *White matter lesions in an unselected cohort of the elderly: molecular pathology suggests origin from chronic hypoperfusion injury.* Stroke, 2006. **37**(6): p. 1391-8.
69. Lahna, D., et al., *Venous Collagenosis as Pathogenesis of White Matter Hyperintensity.* Ann Neurol, 2022. **92**(6): p. 992-1000.

70. Littau, J.L., et al., *Evidence of beta amyloid independent small vessel disease in familial Alzheimer's disease.* Brain Pathol, 2022. **32**(6): p. e13097.
71. Makkinejad, N., et al., *Neuropathological Correlates of White Matter Hyperintensities in Cerebral Amyloid Angiopathy.* J Am Heart Assoc, 2024. **13**(22): p. e035744.
72. McAleese, K.E., et al., *Cortical tau load is associated with white matter hyperintensities.* Acta Neuropathol Commun, 2015. **3**: p. 60.
73. McAleese, K.E., et al., *Extravascular fibrinogen in the white matter of Alzheimer's disease and normal aged brains: implications for fibrinogen as a biomarker for Alzheimer's disease.* Brain Pathol, 2019. **29**(3): p. 414-424.
74. McAleese, K.E., et al., *Frontal white matter lesions in Alzheimer's disease are associated with both small vessel disease and AD-associated cortical pathology.* Acta Neuropathol, 2021. **142**(6): p. 937-950.
75. McAleese, K.E., et al., *Parietal white matter lesions in Alzheimer's disease are associated with cortical neurodegenerative pathology, but not with small vessel disease.* Acta Neuropathol, 2017. **134**(3): p. 459-473.
76. Murray, M.E., et al., *A quantitative postmortem MRI design sensitive to white matter hyperintensity differences and their relationship with underlying pathology.* J Neuropathol Exp Neurol, 2012. **71**(12): p. 1113-22.
77. Pallebage-Gamarallage, M., et al., *Dissecting the pathobiology of altered MRI signal in amyotrophic lateral sclerosis: A post mortem whole brain sampling strategy for the integration of ultra-high-field MRI and quantitative neuropathology.* BMC Neurosci, 2018. **19**(1): p. 11.
78. Roseborough, A.D., et al., *Microvessel stenosis, enlarged perivascular spaces, and fibrinogen deposition are associated with ischemic periventricular white matter hyperintensities.* Brain Pathol, 2022. **32**(1): p. e13017.
79. Silbert, L.C., et al., *White matter hyperintensities and the surrounding normal appearing white matter are associated with water channel disruption in the oldest old.* Alzheimers Dement, 2024. **20**(6): p. 3839-3851.
80. Simpson, J.E., et al., *White matter lesions in an unselected cohort of the elderly: astrocytic, microglial and oligodendrocyte precursor cell responses.* Neuropathol Appl Neurobiol, 2007. **33**(4): p. 410-9.
81. Simpson, J.E., et al., *Microglial activation in white matter lesions and nonlesional white matter of ageing brains.* Neuropathol Appl Neurobiol, 2007. **33**(6): p. 670-83.
82. Smith, C.D., D. Snowdon, and W.R. Markesbery, *Periventricular white matter hyperintensities on MRI: correlation with neuropathologic findings.* J Neuroimaging, 2000. **10**(1): p. 13-6.
83. Solé-Guardia, G., et al., *Association between hypertension and neurovascular inflammation in both normal-appearing white matter and white matter hyperintensities.* Acta Neuropathol Commun, 2023. **11**(1): p. 2.
84. Solé-Guardia, G., et al., *Impact of hypertension on cerebral small vessel disease: A post-mortem study of microvascular pathology from normal-appearing white matter into white matter hyperintensities.* J

Cereb Blood Flow Metab, 2025. **45**(9): p. 1717-1730.

85. Solé-Guardia, G., et al., *Deep learning-based segmentation in MRI-(immuno)histological examination of myelin and axonal damage in normal-appearing white matter and white matter hyperintensities.* Brain Pathol, 2025. **35**(2): p. e13301.
86. Yamamoto, Y., et al., *Neuropathological correlates of temporal pole white matter hyperintensities in CADASIL.* Stroke, 2009. **40**(6): p. 2004-11.
87. Hainsworth, A.H., et al., *Neuropathology of White Matter Lesions, Blood-Brain Barrier Dysfunction, and Dementia.* Stroke, 2017. **48**(10): p. 2799-2804.
88. Huss, A., et al., *Association of Serum GFAP with Functional and Neurocognitive Outcome in Sporadic Small Vessel Disease.* Biomedicines, 2022. **10**(8).
89. Malla, S., et al., *Molecular profiling of frontal and occipital subcortical white matter hyperintensities in Alzheimer's disease.* Front Neurol, 2024. **15**: p. 1470441.
90. Moody, D.M., et al., *Quantification of afferent vessels shows reduced brain vascular density in subjects with leukoaraiosis.* Radiology, 2004. **233**(3): p. 883-90.
91. Shim, Y.S., et al., *Pathological correlates of white matter hyperintensities on magnetic resonance imaging.* Dement Geriatr Cogn Disord, 2015. **39**(1-2): p. 92-104.
92. Lauer, A., et al., *Microbleeds on MRI are associated with microinfarcts on autopsy in cerebral amyloid angiopathy.* Neurology, 2016. **87**(14): p. 1488-1492.
93. Young, V.G., G.M. Halliday, and J.J. Kril, *Neuropathologic correlates of white matter hyperintensities.* Neurology, 2008. **71**(11): p. 804-11.
94. Al-Mashhadi, S., et al., *Oxidative Glial Cell Damage Associated with White Matter Lesions in the Aging Human Brain.* Brain Pathol, 2015. **25**(5): p. 565-74.
95. Chimowitz, M.I., et al., *Further observations on the pathology of subcortical lesions identified on magnetic resonance imaging.* Arch Neurol, 1992. **49**(7): p. 747-52.
96. Desmarais, P., et al., *White matter hyperintensities in autopsy-confirmed frontotemporal lobar degeneration and Alzheimer's disease.* Alzheimers Res Ther, 2021. **13**(1): p. 129.
97. Freeze, W.M., et al., *Corpus callosum lesions are associated with worse cognitive performance in cerebral amyloid angiopathy.* Brain Commun, 2022. **4**(3): p. fcac105.
98. Keith, J., et al., *Collagenosis of the Deep Medullary Veins: An Underrecognized Pathologic Correlate of White Matter Hyperintensities and Periventricular Infarction?* J Neuropathol Exp Neurol, 2017. **76**(4): p. 299-312.
99. Lahna, D., et al., *Postmortem 7T MRI for guided histopathology and evaluation of cerebrovascular disease.* J Neuropathol Exp Neurol, 2022. **82**(1): p. 57-70.
100. McAleese, K.E., et al., *Magnetic resonance imaging of fixed post mortem brains reliably reflects subcortical vascular pathology of frontal, parietal and occipital white matter.* Neuropathol Appl Neurobiol, 2013. **39**(5): p. 485-97.

101. Scheltens, P., et al., *Histopathologic correlates of white matter changes on MRI in Alzheimer's disease and normal aging.* Neurology, 1995. **45**(5): p. 883-8.
102. van Swieten, J.C., et al., *Periventricular lesions in the white matter on magnetic resonance imaging in the elderly. A morphometric correlation with arteriolosclerosis and dilated perivascular spaces.* Brain, 1991. **114 (Pt 2)**: p. 761-74.
103. Scarpelli, M., et al., *MRI and pathological examination of post-mortem brains: the problem of white matter high signal areas.* Neuroradiology, 1994. **36**(5): p. 393-8.
104. Grafton, S.T., et al., *Comparison of postmortem magnetic resonance imaging and neuropathologic findings in the cerebral white matter.* Arch Neurol, 1991. **48**(3): p. 293-8.
105. Raghavan, S., et al., *Vascular risk, gait, behavioral, and plasma indicators of VCID.* Alzheimers Dement, 2024. **20**(2): p. 1201-1213.
106. Rudolph, M.D., et al., *Associations among plasma, MRI, and amyloid PET biomarkers of Alzheimer's disease and related dementias and the impact of health-related comorbidities in a community-dwelling cohort.* Alzheimers Dement, 2024. **20**(6): p. 4159-4173.
107. Sanchez, E., et al., *Association of Plasma Biomarkers With Longitudinal Atrophy and Microvascular Burden on MRI Across Neurodegenerative and Cerebrovascular Diseases.* Neurology, 2025. **104**(7): p. e213438.
108. Sun, Y., et al., *Plasma Neurofilament Light and Longitudinal Progression of White Matter Hyperintensity in Elderly Persons Without Dementia.* J Alzheimers Dis, 2020. **75**(3): p. 729-737.
109. Shir, D., et al., *Association of plasma glial fibrillary acidic protein (GFAP) with neuroimaging of Alzheimer's disease and vascular pathology.* Alzheimers Dement (Amst), 2022. **14**(1): p. e12291.
110. Brickman, A.M., J. Muraskin, and M.E. Zimmerman, *Structural neuroimaging in Altheimer's disease: do white matter hyperintensities matter?* Dialogues Clin Neurosci, 2009. **11**(2): p. 181-90.
111. Wardlaw, J.M., M.C. Valdés Hernández, and S. Muñoz-Maniega, *What are white matter hyperintensities made of? Relevance to vascular cognitive impairment.* J Am Heart Assoc, 2015. **4**(6): p. 001140.
112. Chung, J., et al., *Multimodal Magnetic Resonance Imaging Signatures of White Matter Hyperintensities: Mechanistic Insights Into Pathobiological Heterogeneity.* J Stroke, 2026. **28**(1): p. 1-28.
113. Li, W., et al., *Magnetic susceptibility anisotropy of human brain in vivo and its molecular underpinnings.* Neuroimage, 2012. **59**(3): p. 2088-97.
114. Birkl, C., et al., *The influence of iron oxidation state on quantitative MRI parameters in post mortem human brain.* Neuroimage, 2020. **220**: p. 117080.
115. Birkl, C., et al., *MRI R2* and quantitative susceptibility mapping in brain tissue with extreme iron overload.* Eur Radiol Exp, 2025. **9**(1): p. 80.
116. Qiu, Y., et al., *White matter hyperintensity-associated iron overload links glymphatic system dysfunction to cognitive impairment in cerebral small vessel disease.* Neuroimage, 2025. **321**: p. 121515.

117. Sharma, B., et al., *Brain iron content in cerebral amyloid angiopathy using quantitative susceptibility mapping.* Front Neurosci, 2023. **17**: p. 1139988.
118. Simmons, D.A., et al., *Ferritin accumulation in dystrophic microglia is an early event in the development of Huntington's disease.* Glia, 2007. **55**(10): p. 1074-84.
119. Vymazal, J., D. Urgosík, and J.W. Bulte, *Differentiation between hemosiderin- and ferritin-bound brain iron using nuclear magnetic resonance and magnetic resonance imaging.* Cell Mol Biol (Noisy-le-grand), 2000. **46**(4): p. 835-42.
120. Choo, C.M. and C.H. Tan, *Effects of regional white matter hyperintensities and β-amyloid on domain-specific cognition and progression to dementia.* Brain Cogn, 2025. **188**: p. 106332.
121. Graff-Radford, J., et al., *White matter hyperintensities: relationship to amyloid and tau burden.* Brain, 2019. **142**(8): p. 2483-2491.
122. Kamal, F. and M. Dadar, *Amyloid and tau pathologies are drivers of white matter damage in aging and Alzheimer's disease.* Geroscience, 2026.
123. Pålhaugen, L., et al., *Brain amyloid and vascular risk are related to distinct white matter hyperintensity patterns.* J Cereb Blood Flow Metab, 2021. **41**(5): p. 1162-1174.
124. Weaver, N.A., et al., *Cerebral amyloid burden is associated with white matter hyperintensity location in specific posterior white matter regions.* Neurobiol Aging, 2019. **84**: p. 225-234.
125. Newton, P., et al., *Regional White Matter Hyperintensities and Alzheimer's Disease Biomarkers Among Older Adults with Normal Cognition and Mild Cognitive Impairment.* J Alzheimers Dis, 2023. **92**(1): p. 323-339.

Figures

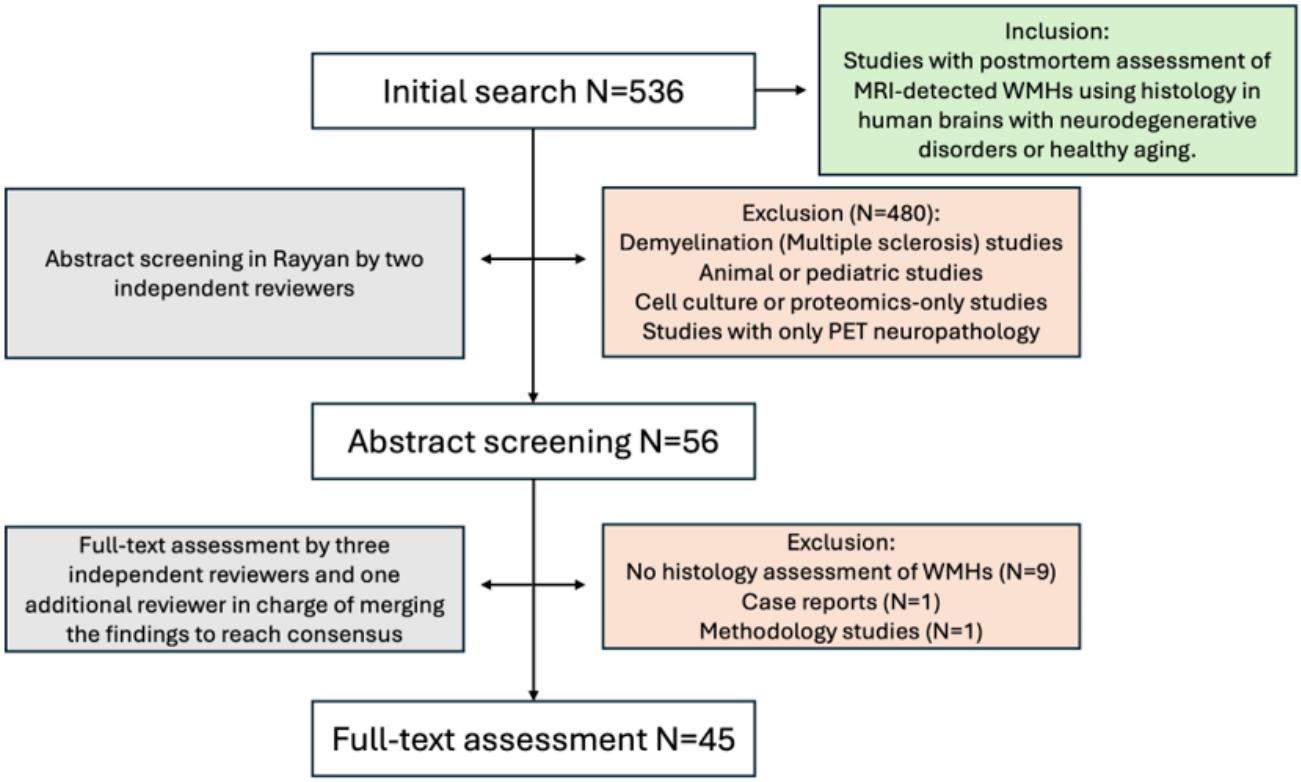


Figure 1

Study selection flowchart. Inclusion and exclusion criteria as well as the number of studies included and excluded in each step. PET=Positron emission tomography imaging.

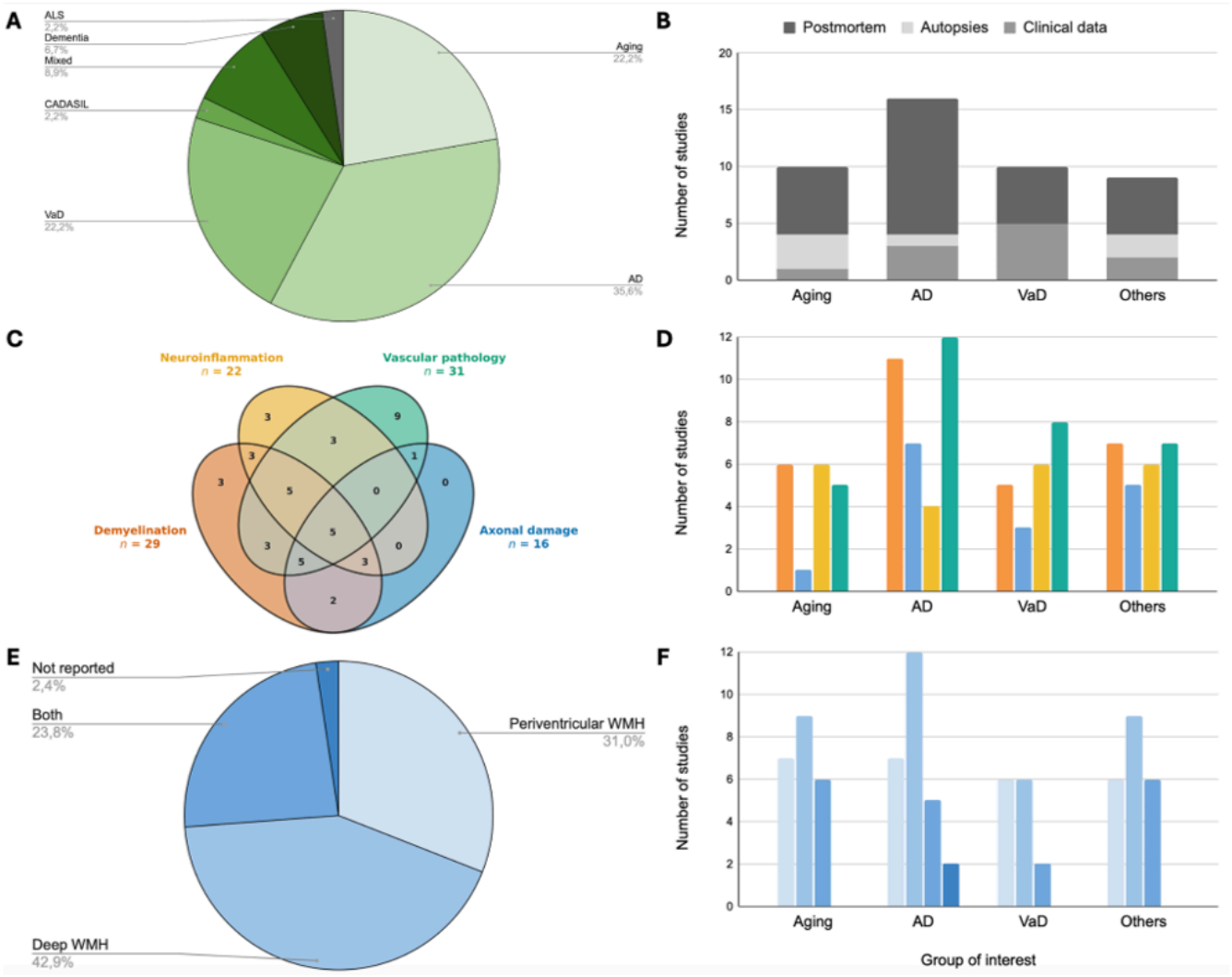


Figure 2

Number of studies included in each category. (A) Percentage of studies assessing each NDD group. (B) Number of studies within each NDD diagnostic group that were either 1-based exclusively on postmortem cohorts (no in vivo data available), 2-involving completed autopsies that may have included access to premortem data, and 3-studies directly correlating postmortem findings with clinical data. (C) Venn diagram showing the number of studies evaluating different histopathological features of vascular pathology (green), demyelination (orange), axonal damage (blue), and neuroinflammation (yellow) as their main contribution. (D) Number of studies within each NDD diagnostic group focusing on the four main histopathological features presented in (C). (E) Percentage of studies differentiating WMH location as pvWMHs, dWMHs, or both. (F) Number of studies within each NDD diagnostic group focusing on the different WMH locations presented in (E). In (B), (D), and (F), “Others” includes studies of dementia, mixed dementia, ALS and CADASIL. CADASIL = Cerebral autosomal dominant arteriopathy with subcortical infarcts and leukoencephalopathy; ALS = amyotrophic lateral sclerosis; AD = Alzheimer’s disease; VaD = vascular dementia.

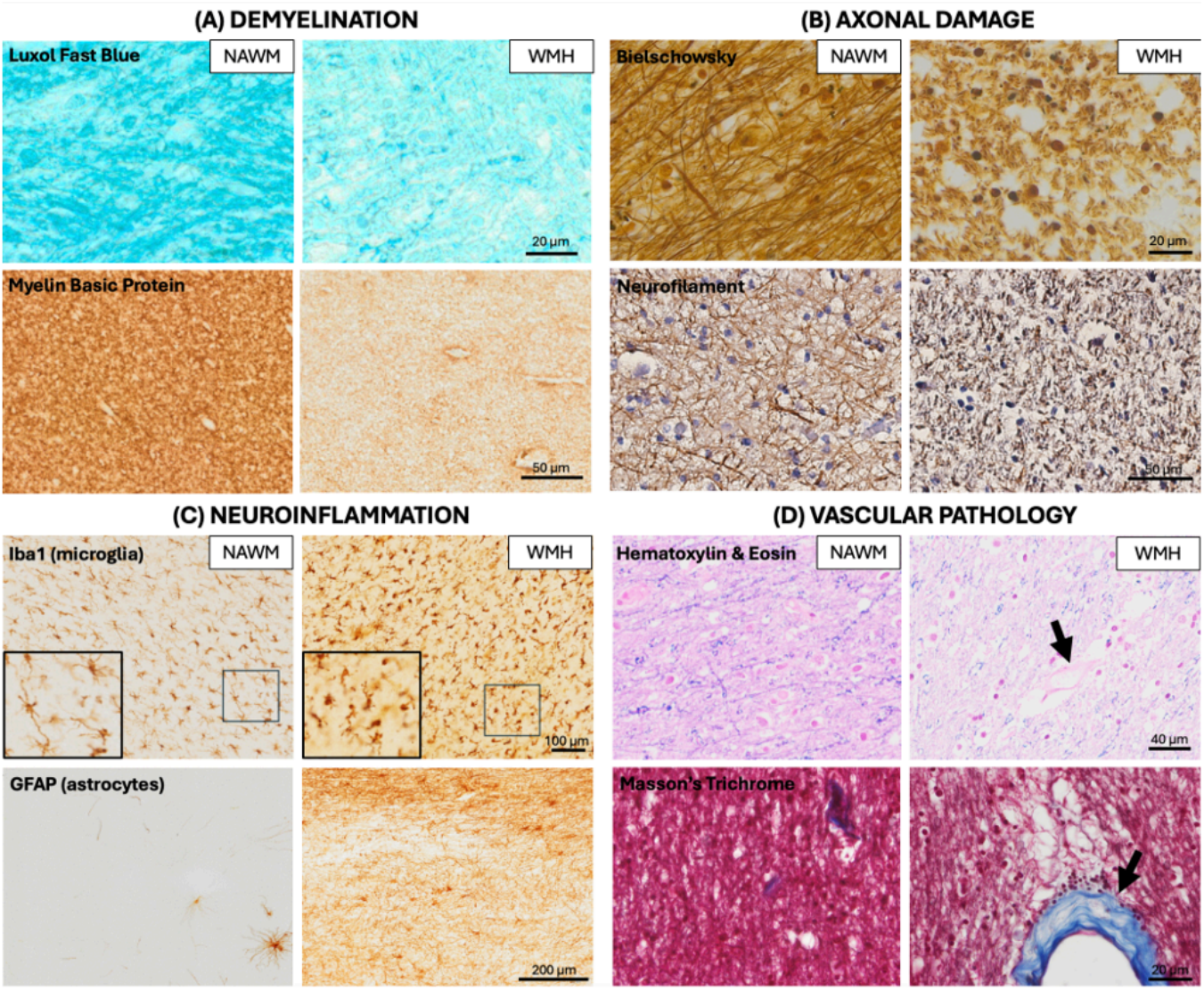


Figure 3

Most widely used staining types to evaluate white matter hyperintensity histopathology features. (A) Stains used to evaluate demyelination, including Luxol Fast blue and immunohistochemistry for Myelin Basic Protein. Both staining types show reduced labeling intensity of myelin fibers in white matter hyperintensities (right) compared to normal-appearing white matter (left). (B) Stains used to evaluate axonal damage, including Bielschowsky silver stain and immunohistochemistry for neurofilament. Both staining types show reduced axonal staining intensity, tissue damage and loss of directionality in the fibers' orientation in white matter hyperintensities (right) compared to normal-appearing white matter (left). (C) Stains used to evaluate neuroinflammation, including immunohistochemistry for Iba1 (microglia) and GFAP (astrocytes), both showing changes in the cells' morphology (inserts) in white matter hyperintensities (right) compared to normal-appearing white matter (left), reflecting their activation. (D) Stains used to evaluate the vascular pathology (and also global tissue integrity), including H&E and Masson's Trichrome. Both staining types show the vascular wall of blood vessels (i.e., endothelial cells and muscle actin in H&E, and collagen stained in blue in Masson's Trichrome, both features indicated with black arrows). Scale bars are valid for both NAWM and WMH photomicrographs.

All photomicrographs were acquired in slides of WMHs blocks that have been processed in our laboratory.

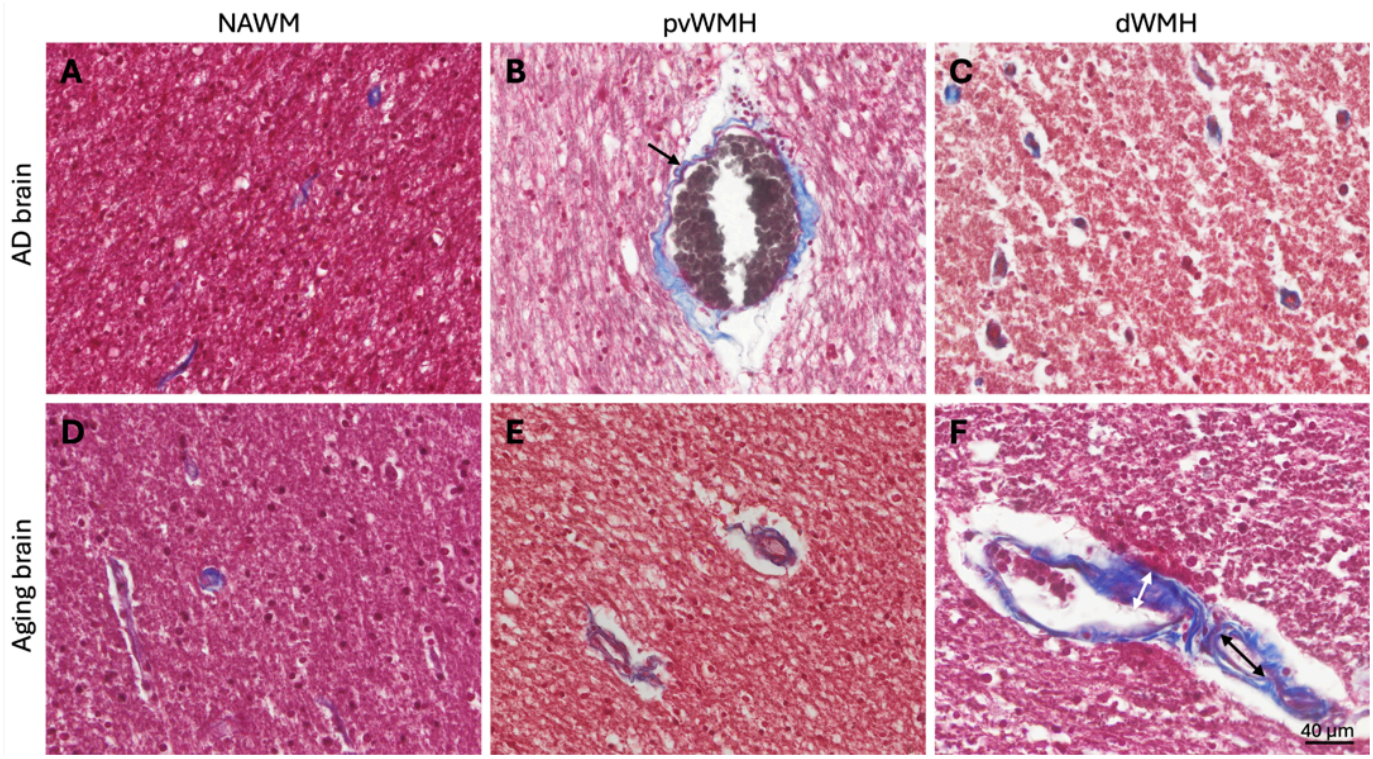


Figure 4

Masson's Trichrome staining in one Alzheimer's disease specimen and in one aging brain, showing periventricular and deep white matter hyperintensities compared to normal-appearing white matter. One AD brain within (A) NAWM; (B) pvWMH showing a tortuous vessel wall and a remaining blood clot in the lumen; and (C) dWMH showing multiple microvessels with collagen within WM spongiosis. Aging brain within (D) NAWM; (E) pvWMH with two microvessels; and (F) dWMH with increased collagen thickness (white arrow) and reduced lumen (black arrow). Scale bar=40µm. AD=Alzheimer's disease; NAWM=Normal-appearing white matter; pvWMH=periventricular white matter hyperintensity; dWMH=deep WMH. All photomicrographs were acquired in slides of WMHs blocks that have been processed in our laboratory.

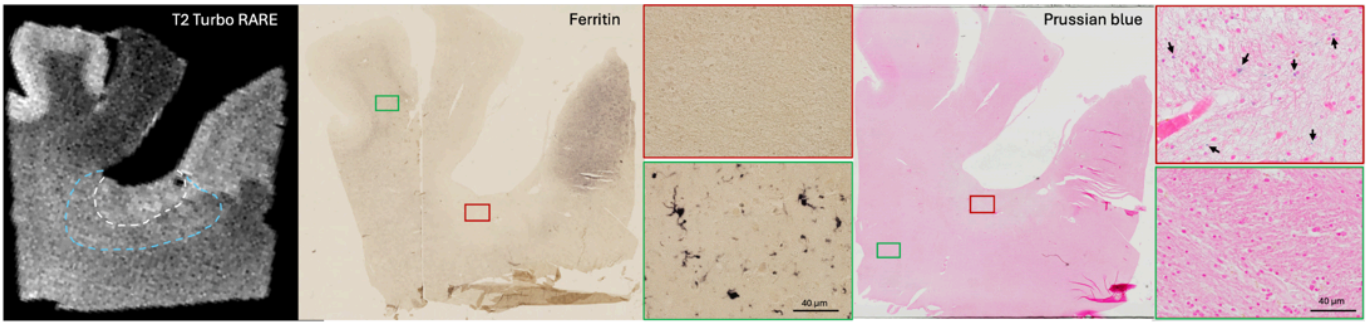


Figure 5

Iron histology of pvWMHs compared to NAWM. T2 TurboRare MRI shows the core WMH lesion (white dotted lines) and the perilesional hyperintensity (blue dotted lines). Immunohistochemistry of ferritin photomicrographs has been registered to the MRI, showing macrophages in NAWM, but not in WMHs. Prussian blue staining (hemosiderin) shows iron deposits in blue (black arrows) in WMHs but not in NAWM. MRI and photomicrographs were acquired in WMHs blocks that have been processed in our laboratory.